



National Technical University of Athens  
School of Naval Architecture and Marine  
Engineering  
Laboratory of Marine Engineering

LNG Carrier COGES System: Technoeconomic and Environmental model based  
assessment.

Diploma Thesis  
of  
**Ioannis Kourelis**

Supervisor: Associate Professor Dimopoulos George



Εθνικό Μετσόβειο Πολυτεχνείο  
Σχολή Ναυπηγών Μηχανολόγων Μηχανικών  
Εργαστήριο Ναυτικής Μηχανολογίας

Τεχνοοικονομική και Περιβαλλοντική Αξιολόγηση Πλοίου Μεταφοράς  
Υγροποιημένου Φυσικού Αερίου με Συνδιασμένο Σύστημα Αεριοστρόβιλου και  
Ηλεκτροπαραγωγού Ατμοστρόβιλου: Μοντελοποίηση και Ανάλυση.

Διπλωματική Εργασία

του

**Ιωάννη Κουρελή**

Επιβλέπων: Αναπληρωτής Καθηγητής Δημόπουλος Γεώργιος



## Table of Contents

List of Figures .....	5
List of Tables .....	6
Acknowledgments.....	8
Introduction .....	9
Abstract .....	9
Motivation.....	9
Structure of Thesis.....	10
Decarbonization and New Technologies.....	10
LNG .....	10
Regulations .....	11
Arrangement History and Existing Technologies.....	12
New Technologies .....	13
Detailed Description of the COGES System .....	14
COGES Arrangement Representation .....	14
Main Differences between COGES and 2-stroke DFM in LNG Carriers .....	14
Describing the Simulation.....	15
gPROMS Model Builder 7.1.1.....	15
Model Ship Main Characteristics.....	16
Conventional LNG Carrier Model .....	17
COGES System .....	30
Analysis of Results Table .....	33
Simulation Results .....	34
Initial Test .....	34
Initial Test Comparisons through the Roundtrips .....	39
Analysis of the Roundtrips .....	39
Initial Test Results .....	42
Analysis of COGES System's Alterations.....	44
Presentation of Cases .....	45
Cases Analysis .....	45
Case 1 .....	46
Case 2.....	47
Case 3.....	48
Case 4.....	48
Case 5.....	49
Case 6.....	49

Case 7 .....	50
Case 8 .....	51
Cases 9-12 .....	51
Conclusions.....	57
References.....	58
Data Tables .....	60

## List of Figures

Figure 1: LNG Carrier .....	9
Figure 2: LNG Composition .....	10
Figure 3: Emission Control Areas.....	11
Figure 4: Methane Pioneer .....	12
Figure 5: Arrangement of conventional 2 stroke DF engine propulsion system in LNG carrier.....	13
Figure 6: Combined Gas Turbine Electric and Steam System Arrangement .....	14
Figure 7: gPROMS Model Builder 7.1.1 .....	15
Figure 8: Propulsion Demand (Ballast Condition).....	16
Figure 9: Propulsion Demand (Laden Condition) .....	16
Figure 10: Conventional LNG Propulsion Model in GPROMS Interface .....	17
Figure 11: MAN 5G70ME-C10-GI Dual Fuel Engine.....	17
Figure 12: Results Names for Conventional LNGC Model .....	29
Figure 13: Coding of the "Results" Table in GPROMS Language for Conventional LNGC Model .....	29
Figure 14: COGES System Propulsion Model in GPROMS Interface .....	30
Figure 15: Data Input for HRSG System.....	30
Figure 16: Data Input for W10V31SG .....	31
Figure 17: Data Input for SGT400 .....	31
Figure 18: Data Input for Steam Turbine.....	32
Figure 19: Results Names for COGES System Model.....	32
Figure 20: Coding of the "Results" Table in GPROMS Language for COGES System Model .....	32
Figure 21: Cargo Consumption per Day.....	34
Figure 22: Total Energy Consumption per Day .....	35
Figure 23: System Efficiency.....	35
Figure 24: Ship Efficiency.....	36
Figure 25: R Cargo Consumed.....	36
Figure 26: R Propulsion .....	37
Figure 27: R Parasitic .....	37
Figure 28: R GCU.....	38
Figure 29: USA - Europe Trip .....	39

Figure 30: USA - Asia Trip.....	41
Figure 31: Cargo Consumption per Year (USA - EU Trip) .....	43
Figure 32: Cargo Consumption per Year (USA - ASIA Trip).....	43
Figure 33: Case 1 Results for US-EUR Trip.....	46
Figure 34: Case 1 Results for US - ASIA Trip .....	46
Figure 35: Case 2 Results for US-EUR Trip.....	47
Figure 36: Case 2 Results for US - ASIA Trip .....	47
Figure 37: Features of Cases 9-12.....	51

## List of Tables

Table 1: Main Engine model explanatory table .....	18
Table 2: Main Engine Gas Mode Performance Table.....	19
Table 3: Main Engine Gas Mode Table of Capacities .....	20
Table 4: Main Engine Fuel Mode Performance Table.....	21
Table 5: 6L34DF Engine Capacity Data (Gas Mode).....	22
Table 6: 6L34DF Generator Performance Data (Gas Mode) (1).....	23
Table 7: 6L34DF Generator Performance Data (Gas Mode) (2).....	23
Table 8: 6L34DF Engine Capacity Data (Liquid Fuel Mode).....	24
Table 9: 6L34DF Generator Performance Data (Liquid Fuel Mode) (1).....	24
Table 10: 6L34DF Generator Performance Data (Liquid Fuel Mode) (2).....	25
Table 11: 8L34DF Engine Capacity Data (Gas Mode).....	25
Table 12: 8L34DF Generator Performance Data (Gas Mode) (1).....	26
Table 13: 8L34DF Generator Performance Data (Gas Mode) (2).....	26
Table 14: 8L34DF Engine Capacity Data (Liquid Fuel Mode).....	27
Table 15: 8L34DF Generator Performance Data (Liquid Fuel Mode) (1).....	27
Table 16: 8L34DF Generator Performance Data (Liquid Fuel Mode) (2).....	28
Table 17: 5G70ME-C10-GI 2-stroke Engine Performance Table .....	28
Table 18: 6L34DF Auxiliary Engine Performance Table.....	28
Table 19: 8L34DF Auxiliary Engine Performance Table.....	28
Table 20: Table of time spent on each velocity for the USA-EU Trip.....	40
Table 21: Table of time spent on each velocity for the USA-Asia Trip.....	41
Table 22: Results for the USA - Europe Trip.....	42
Table 23: Results for the USA - Asia Trip .....	43
Table 24: Case 3 Results .....	48
Table 25: Case 4 Results .....	48
Table 26: Case 5 Results .....	49
Table 27: Case 6 Results .....	49
Table 28: Case 7 Results .....	50
Table 29: Case 8 Results .....	51
Table 30: Case 9-12 Results for US - EUR Trip (1).....	52
Table 31: Case 9-12 Results for US - EUR Trip (2).....	53
Table 32: Case 9-12 Results for US - ASIA Trip (1).....	54

Table 33: Case 9-12 Results for US - ASIA Trip (2) .....	55
Table 34: Conventional LNGC without Shaft Generator Data Table .....	60
Table 35: Conventional LNGC with Shaft Generator Data Table.....	60
Table 36: COGES System Initial Test Data Table .....	60
Table 37: Case 1 Data Table .....	61
Table 38: Case 2 Data Table .....	61
Table 39: Case 3 Data Table .....	61
Table 40: Case 4 Data Table .....	62
Table 41: Case 5 Data Table .....	62
Table 42: Case 6 Data Table .....	62
Table 43: Case 7 Data Table .....	63
Table 44: Case 8 Data Table .....	63
Table 45: Case 9 Data Table .....	63
Table 46: Case 10 Data Table .....	64
Table 47: Case 11 Data Table .....	64
Table 48: Case 12 Data Table .....	64

## Acknowledgments

This thesis marks the completion of my undergraduate studies at the School of Naval Architecture and Marine Engineering of the National Technical University of Athens. It has been a long journey, at times challenging, but undoubtedly rewarding, during which I acquired valuable knowledge and experiences. I would first like to express my deepest gratitude to my family, whose unwavering support and encouragement throughout all these years have been instrumental in reaching this point. Their belief in me gave me strength in every step of the way. I am also sincerely thankful to all the professors of the School for the knowledge they shared and their guidance throughout my studies. In particular, I would like to thank Professor Georgios Dimopoulos for his insightful guidance, patience, and support during the development of my diploma thesis. Lastly, I would like to express my warmest thanks to Mr. Nikolaos Grivas, Technical Manager at MINERVA GAS Inc., for his kind assistance and for providing essential data related to one of the company's vessels, which greatly contributed to the quality and depth of my research.

# Introduction

## Abstract

The European Union has set an ambitious goal of achieving net-zero CO<sub>2</sub> emissions by 2050. This transition significantly impacts the maritime industry, the world's largest transportation sector. As a result, stringent greenhouse gas (GHG) emission reduction requirements have forced companies to invest millions in sustainable solutions. Extensive research has been conducted on new technologies and alternative fuels to support this transition while keeping the financial results sustainable. This Diploma Thesis aims to evaluate and analyze advanced technologies that contribute to maritime decarbonization, with a particular focus on the Combined Gas Turbine Electric and Steam (COGES) system used in the place of the traditional 2-stroke Dual Fuel Engine for propulsion on LNG carriers.



*Figure 1: LNG Carrier*

## Motivation

As previously stated, the IMO has implemented an initial strategy targeting a significant reduction in total GHG emissions by 2050. In order to achieve that, there have been many researches investigating new technologies for optimized technical and operational efficiency. Through the analysis that will be conducted it will be determined whether the COGES System can replace the conventional 2-stroke DFM (Dual Fuel Mechanical) engines in modern LNG carriers. The criteria by which this will be judged are a variety of measurements regarding fuel oil consumption, the overall ship's efficiency, GHG emissions per cubic meters of cargo transported and the ship's general environmental footprint.

## Structure of Thesis

The current study will be structured as it follows. Firstly, the decarbonization problem will be discussed as well as propulsion technologies, fuels and regulations linked with modern LNG carriers. More explicitly, a presentation of new ideas for the propulsion arrangements will occur, in which a brief introduction of the Combined Gas Turbine Electric and Steam (COGES) system will be mentioned after a historical review of the LNG propulsion configurations over the years. After this introduction, the specifications of our case study will be examined, with a comprehensive look in the data description of the conventional LNG carrier as well as the model based ship case. Furthermore, the next chapter is consisted of the simulation campaign, variety of graphics and brief comments on each result of the simulation. Last but not least, the results of the simulations will be presented accompanied by a thermo-economic assessment of the problem, depending on real time cost of fuel, cost of CO<sub>2</sub>/ton of fuel for two existing voyages.

## Decarbonization and New Technologies

### LNG

Liquefied Natural Gas (LNG) is a widely used alternative fuel in modern shipping. It primarily consists of methane (CH<sub>4</sub>), making up 85% to 95% of its composition, along with smaller amounts of ethane, propane, butane, and nitrogen. This fuel is both colorless and odorless and is produced by cooling natural gas to a temperature of -161°C, at atmospheric pressure. Figure 1 indicates a typical composition of LNG. A crucial aspect of natural gas transportation is converting it into a liquid state, as LNG takes up only 1/600th of its original volume, making storage and transport far more efficient. LNG has emerged as the primary competitor to Heavy Fuel Oil (HFO) in the maritime sector due to its ability to drastically cut emissions. It can reduce sulfur oxides (SO<sub>x</sub>) by nearly 100%, nitrogen oxides (NO<sub>x</sub>) by up to 85%, and also minimizes particulate matter. One of the greatest advantages of adopting LNG is that the existing global infrastructure can quickly adapt to support its bunkering and supply needs. However, the issue of methane slip cannot be overlooked when discussing LNG. Methane slip refers to the unburned methane that escapes into the atmosphere during the combustion process in engines and gas systems (*Methane Slip*, n.d.). Since methane (CH<sub>4</sub>) is a greenhouse gas with a significantly higher global warming potential than CO<sub>2</sub>, its release can have a considerable environmental impact, sometimes outweighing the benefits of reduced carbon dioxide emissions (*LNG Composition*, 2024).

Element	Unit	
N <sub>2</sub> (Nitrogen)	% mol.	0.12
CH <sub>4</sub> (Methane)	% mol.	93.77
C <sub>2</sub> H <sub>6</sub> (Ethane)	% mol.	3.80
C <sub>3</sub> H <sub>8</sub> (Propane)	% mol.	1.67
I-C <sub>4</sub> H <sub>10</sub> (Iso-Butane)	% mol.	0.29
N-C <sub>4</sub> H <sub>10</sub> (Normal-Butane)	% mol.	0.32
I-C <sub>5</sub> H <sub>12</sub> (Iso-Pentane)	% mol.	0.02

Figure 2: LNG Composition



## Arrangement History and Existing Technologies

In 1959, Methane Pioneer, a 5500 cubic meters LNG carrier set sail from the Louisiana Gulf heading to the UK becoming the first vessel to transport Liquefied Natural Gas. It was equipped with a Steam Turbine propulsion system, using boil-off gas as a supplementary fuel for its steam boilers. The steam generators on board featured combined burners capable of operating on a single fuel, either heavy fuel oil (HFO) or gas or a combination of both, allowing flexibility in fuel selection. The main steam flow produced in the burners was distributed to all steam turbines within the propulsion plant, including both the main propulsion turbines and auxiliary turbines, ensuring efficient power generation and operation of essential onboard systems (*Methane Pioneer: The First LNG Ship in the World*, 2012).



Figure 4: Methane Pioneer

In the early 2000s, Diesel-electric propulsion became a significant advancement in LNG carrier technology offering improved fuel efficiency and operational flexibility compared to traditional steam turbine systems. In this arrangement, multiple medium-speed diesel or dual-fuel engines generate electricity, which powers electric propulsion motors connected to the ship's propellers. This system, known as Dual-Fuel Diesel-Electric (DFDE), allowed LNG carriers to use boil-off gas (BOG) as fuel, reducing dependence on heavy fuel oil. DFDE propulsion provided better part-load efficiency, enhanced maneuverability, and lower fuel consumption, making it a popular choice for LNG shipping. However, despite these advantages, DFDE ships had higher maintenance requirements and methane slip issues due to the Otto-cycle combustion process used in dual-fuel engines. As the industry sought even greater efficiency and lower emissions, attention shifted toward two-stroke dual-fuel engines, which offered improved thermal efficiency and reduced methane slip. The introduction of dual-fuel two-stroke engines marked a significant leap in LNG carrier propulsion, offering higher efficiency and lower emissions compared to both steam turbines and diesel-electric systems. Two main technologies emerged: MAN Energy Solutions' ME-GI (Gas Injection) engines, which operate on a Diesel-cycle, and WinGD's X-DF engines, which use an Otto-cycle combustion process (*MEGI Two Stroke Engines*, 2025) (*X-DF Dual-Fuel Design*, 2025). These engines can run on boil-off gas (BOG) or conventional marine fuels, providing fuel flexibility while significantly reducing fuel consumption and CO<sub>2</sub> emissions.

As illustrated in the diagram below, a typical two-stroke engine propulsion system used on LNG carriers includes two High Duty (HD) compressors, four electric generators, two main engines, a reliquefaction (RLQ) system, a Gas Combustion Unit (GCU), and a boiler. The system operates by processing the Boil-Off Gas (BOG) through the Fuel Gas Handling System (FGHS), which monitors and matches the amount of fuel required by the engines

and generators with the fuel supplied. The BOG is then distributed through the system to generate steam, electrical power for the entire vessel, and mechanical power for the propellers. Any excess BOG not processed by the RLQ system is redirected to the GCU. In cases where naturally occurring BOG is insufficient, the FGHS activates an LNG pump and Fuel Evaporator to produce Forced Boil-Off Gas (FBOG) to meet the ship's energy demands. Additionally, a Heavy Fuel Oil (HFO) tank supplies pilot fuel for both the engines and generators.

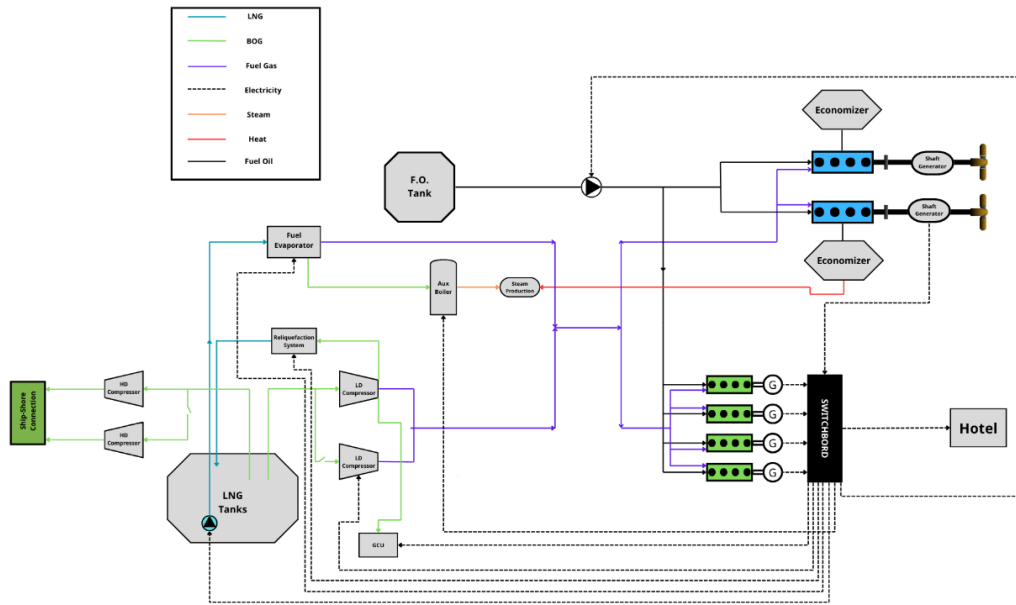


Figure 5: Arrangement of conventional 2 stroke DF engine propulsion system in LNG carrier

## New Technologies

The drive for greater efficiency and lower emissions in LNG carrier propulsion has led to the adoption of innovative technologies. Hybrid-electric systems with battery storage (BESS) help optimize fuel consumption, while air lubrication systems (ALS) reduce hull resistance, improving efficiency. Wind-assisted propulsion, using rotor sails and kites, is also being explored to cut fuel use. Additionally, the industry is investing in alternative fuels like bio-LNG, synthetic LNG, ammonia, and hydrogen to support decarbonization. Among these advancements, COGES (Combined Gas Turbine Electric and Steam) systems stand out for their high efficiency, fuel flexibility, and waste heat recovery, making them a promising solution for the future of LNG carrier propulsion.

## Detailed Description of the COGES System

### COGES Arrangement Representation

This propulsion system is a possible solution for the maritime industry in the future. COGES system includes the reliquefaction system and the GCU just as the conventional model, two generators operating with compressed BOG from the low duty compressors combined with fuel oil from the fuel tanks as well as the main unit. The compressor receives BOG from the LNG tanks, the compressed gas along with air goes into the combustion chamber and the exhaust gas spin the gas turbine. Since the exhaust gas has an average temperature of 500 °C after the gas turbine, there is a Heat Recovery Steam Generator in order to produce additional electricity. In conclusion, an Electric Energy Storage (EES) is present which further drives a steam turbine for additional power generation.

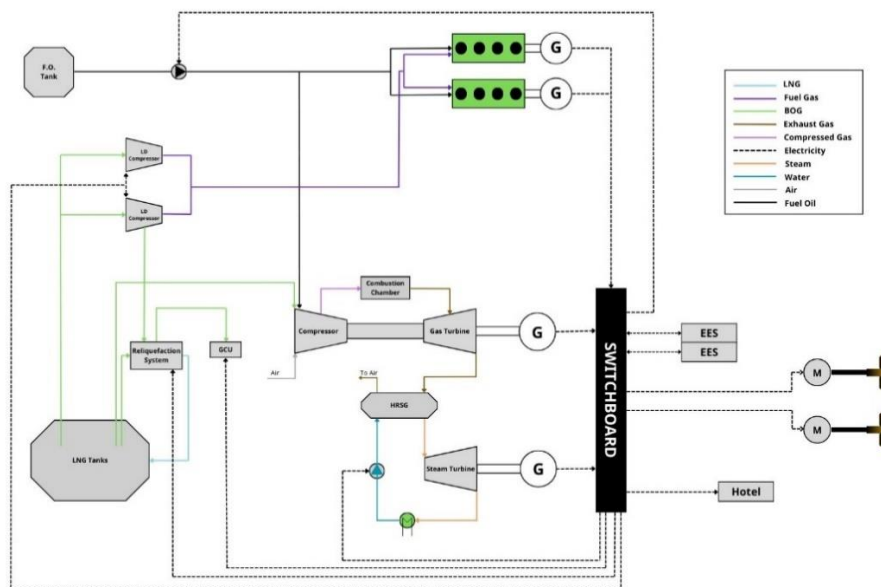


Figure 6: Combined Gas Turbine Electric and Steam System Arrangement

### Main Differences between COGES and 2-stroke DFM in LNG Carriers

Despite their propulsion architecture, the main difference between the COGES system and the conventional two-stroke dual-fuel mechanical (DFM) engine lies in their energy conversion methods. The COGES system results in a fully electric propulsion with high thermal efficiency and reduced emissions. In contrast, a two-stroke DF engine is a direct mechanical drive system, where the reciprocating engine burns LNG or fuel oil to produce mechanical power that directly drives the propeller through a reduction gear or shaft system. Conventional 2-stroke DFM engines produce higher  $\text{NO}_x$  and particulate emissions compared to a COGES system, which also benefits from having no methane slip. Additionally, COGES systems offer lower vibration and reduced maintenance needs. Finally, yet importantly, the COGES system occupies significantly lower volume than the DFM inside the engine room because the first one does not acquire two long shafts

connected to the propulsion system and also, the whole volume of the installation is a lot smaller than the one used in the conventional LNGC. These two aspects are crucial to COGES propulsion, as they allow vessels to accommodate more cargo while also reducing the hydrodynamic resistance of the hull. Traditionally, ships required a bulkier hull design to accommodate the large machinery room, engine, and shafts. With COGES, the elimination of these constraints results in a more streamlined hull and increased cargo capacity. However, a big drawback is that such a system has more expensive installation. Most LNG carriers operating today, implement the conventional propulsion method and therefore the cost for the ship owners of switching to COGES propulsion is very high.

## Describing the Simulation

### gPROMS Model Builder 7.1.1

In this study, gPROMS by Siemens Process Systems Enterprise is utilized as a powerful equation-oriented modeling and simulation environment to compare the performance of a conventional LNG carrier with that of a similar vessel equipped with a COGES. The program gPROMS enables the development of high-fidelity, first-principles models that incorporate thermodynamic, operational, and environmental parameters. Its capabilities in dynamic simulation, parameter estimation, and steady-state optimization allow for a comprehensive technoeconomic and environmental assessment under realistic operating conditions. This model-based approach is particularly well-suited for evaluating complex energy systems where fuel efficiency, emissions, and transient behavior are critical. (*gPROMS Digital Process Design and Operation*, 2025)



Figure 7: gPROMS Model Builder 7.1.1

The models employed in this analysis are sourced from a validated database developed by the National Technical University of Athens (NTUA), ensuring both accuracy and relevance to marine propulsion systems. Advanced tools for uncertainty analysis, scenario-based optimization, and multi-domain integration of the program enable a detailed investigation of the performance trade-offs between conventional and COGES configurations. Through this modeling framework, the study provides data-driven insights into the potential benefits of adopting COGES technology on LNG carriers in terms of fuel savings, emissions reduction, and lifecycle performance (Dimopoulos, G., Georgopoulou, C., Stefanatos, J., 2019).

## Model Ship Main Characteristics

Both simulations of the research are conducted on the same ship in order to provide comparable and acceptable results and come to sufficient conclusions. The data for the ship's dimensions and main characteristics were drawn from a vessel from a shipping company.

The vessel has length between perpendiculars equal to 295 m, is 46 m wide and for our model simulation sails with an operating speed of 14.9 kn at 12 m draft. The ship can transport 174.000 m<sup>3</sup> of LNG and has a boil-off rate approximately equal to 0.082% (3535kg/h). In the table below the Power/Speed curves of the vessel are shown.

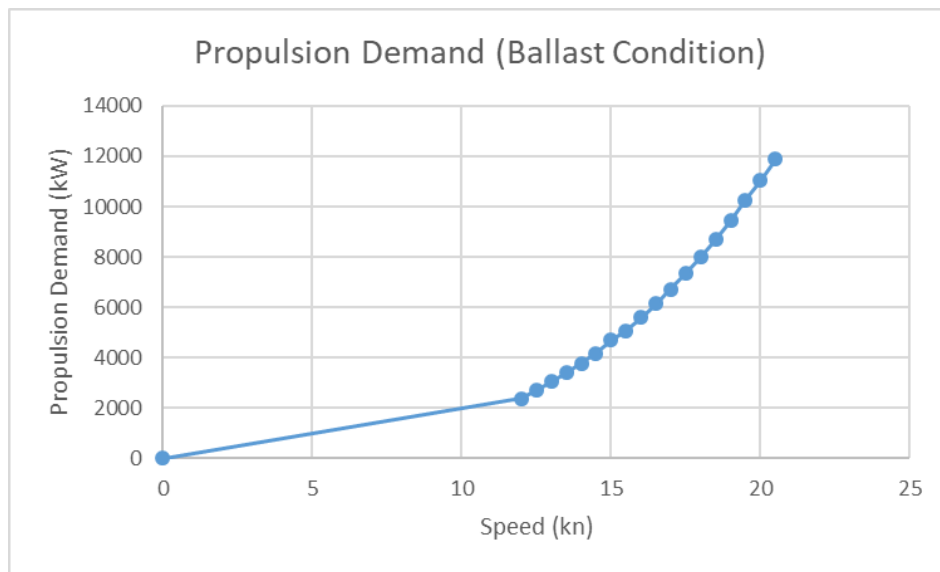


Figure 8: Propulsion Demand (Ballast Condition)

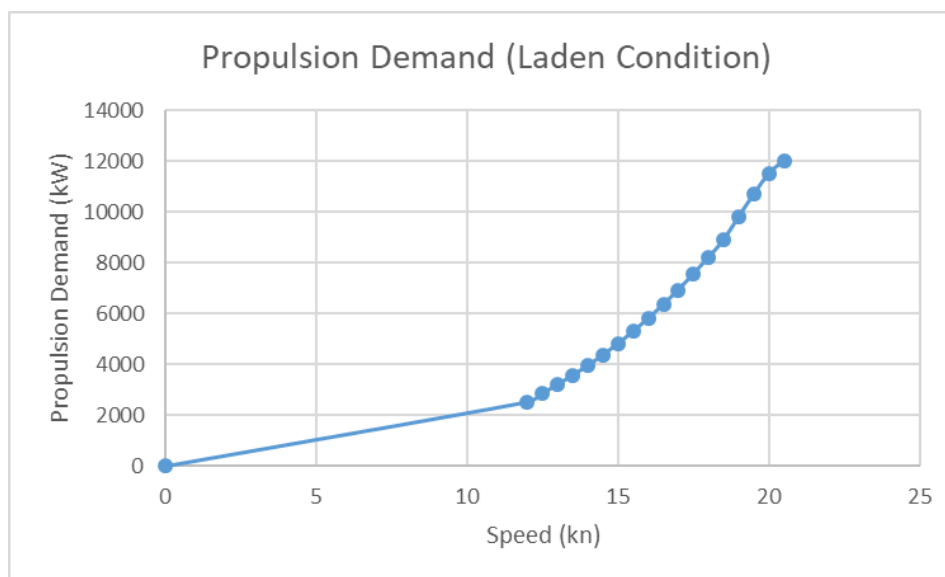


Figure 9: Propulsion Demand (Laden Condition)

Before presenting the different characteristics of the two models it is important to note that the model using the COGES propulsion system is capable of transporting more LNG than the conventional model.

### Conventional LNG Carrier Model

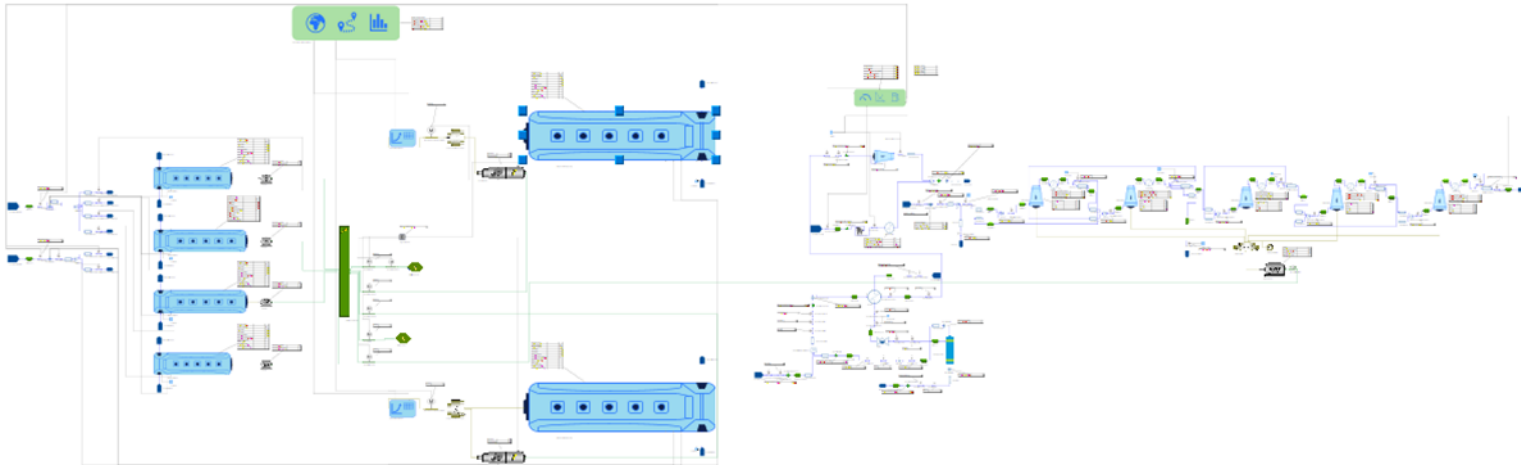


Figure 10: Conventional LNG Propulsion Model in GPROMS Interface

The conventional LNGC is equipped with two 5G70ME-C10-GI 2-stroke engines from MAN-B&W group. Each engine has an MCR of 12,590 kW at 69 rpm. It is also equipped with two 6L34DF and two 8L34DF WARTSILA electrical generators with an MCR of 2,880 kW and 3,840 kW, respectively. In order to introduce the main engine's and generator's data into the program it is essential to convert them into the required format.



Figure 11: MAN 5G70ME-C10-GI Dual Fuel Engine

The first task that has to be completed is to calculate on an excel sheet the following variables. The data for these variables were drawn from the manual of the engines:

Load	Engine load
"Speed"	Engine speed
"BSFC LFM"	BSFC Fuel Oil mode
"BSFC GFM"	BSFC Gas mode
"BSFC PLT"	BSFC pilot Fuel
MFLair GFM	Mass flow air
"Texh GFM"	Temperature exhaust gas
"TaC GFM"	Temperature air after T/C compressor
"Tscav GFM"	Temperature scavenging
"Pscav GFM"	Pressure scav.
"Qcac GFM"	Heat dissipation scav. air cooler
"Qjct GFM"	Heat dissipation Jacket
"Qlub GFM"	Heat dissipation Lub. oil
MFLair LFM	Mass flow air
"Texh LFM"	Temperature exhaust gas
"TaC LFM"	Temperature air after T/C compressor
"Tscav LFM"	Temperature scavenging
"Pscav LFM"	Pressure scav.
"Qcac LFM"	Heat dissipation scav. air cooler
"Qjct LFM"	Heat dissipation Jacket
"Qlub LFM"	Heat dissipation Lub. oil

*Table 1: Main Engine model explanatory table*

The performance table created is the key basic input for the GPROMS program. The same process is repeated for the two pairs of auxiliary engines. To deal with the complex calculations, important data from the engine manual is presented, which will later be applied in the experimental process. All of the information is derived from the MAN manual for the main engine (*G70ME-C10\_5-GI*, 2025).

Low Flashpoint Fuel (TIER III) ISO CONDITIONS								
Load	Power	Speed	SPOC	SGC	Heat rate	Exh.gas amount	Exh.gas temperature	Steam
%SMCR	kW	r/min	g/kWh	g/kWh	kJ/kWh	kg/s	°C	kg/h
100	12590.0	69.0	2.67	134.8	6.9	25.8	222.0	1148.0
95	11961.0	67.8	2.76	133.7	6.8	25.0	215.0	997.0
90	11331.0	66.6	2.86	132.8	6.8	24.2	210.0	871.0
85	10702.0	65.4	2.98	132.1	6.7	23.2	206.0	769.0
80	10072.0	64.1	3.10	132.0	6.7	22.2	204.0	695.0
75	9443.0	62.7	3.24	132.0	6.7	21.3	202.0	655.0
70	8813.0	61.3	3.39	130.7	6.7	20.1	203.0	636.0
65	8184.0	59.8	3.56	129.8	6.6	18.9	204.0	638.0
60	7554.0	58.2	3.75	130.0	6.7	17.8	206.0	635.0
55	6925.0	56.5	3.98	130.3	6.7	16.7	205.0	594.0
50	6295.0	54.8	4.24	130.8	6.7	15.5	206.0	580.0
45	5666.0	52.9	4.55	131.5	6.8	14.2	213.0	644.0
40	5036.0	50.8	4.92	132.4	6.8	14.3	186.0	259.0
35	4407.0	48.6	5.37	133.2	6.9	12.9	188.0	274.0
30	3777.0	46.2	5.96	134.0	7.0	10.6	207.0	457.0
25	3148.0	43.5	6.73	134.8	7.0	8.5	220.0	514.0
20	2519.0	40.8	7.50	135.6	7.1	6.4	233.0	571.0
15	1890.0	38.1	8.27	136.4	7.2	4.3	246.0	628.0
10	1261.0	35.4	9.04	137.2	7.2	2.2	259.0	685.0

Table 2: Main Engine Gas Mode Performance Table

**Table of Capacities , Low Flashpoint Fuel, ISO CONDITIONS**

<b>Load</b>	<b>T/C air consumption +-5%</b>	<b>Scavenge air pressure</b>	<b>Scavenge air receiver temp</b>	<b>Scavenge air heat diss.</b>	<b>Jacket water heat diss +10/-15%</b>	<b>Lubricating oil heat diss +-10%</b>	<b>Vaporizer heat</b>	<b>Condensed Water</b>
<b>%SMCR</b>	<b>kg/s</b>	<b>bara</b>	<b>°C</b>	<b>kW</b>	<b>kW</b>	<b>kW</b>	<b>kW</b>	<b>t/24h</b>
100	25.3	4.15	37.0	4410.0	1680.0	1020.0	370.0	0.0
95	24.5	3.99	36.0	4120.0	1620.0	980.0	349.0	0.0
90	23.7	3.82	35.0	3830.0	1550.0	940.0	328.0	0.0
85	22.8	3.62	34.0	3500.0	1490.0	900.0	308.0	0.0
80	21.8	3.47	33.0	3220.0	1430.0	860.0	290.0	0.0
75	21.0	3.35	32.0	2990.0	1370.0	820.0	272.0	0.0
70	19.8	3.12	31.0	2630.0	1310.0	780.0	251.0	0.0
65	18.6	2.88	30.0	2280.0	1240.0	750.0	232.0	0.0
60	17.5	2.68	30.0	1980.0	1180.0	710.0	214.0	0.0
55	16.4	2.47	29.0	1700.0	1120.0	680.0	197.0	0.0
50	15.3	2.26	28.0	1420.0	1060.0	640.0	179.0	0.0
45	14.0	2.09	27.0	1160.0	990.0	600.0	163.0	0.0
40	14.1	2.02	26.0	1130.0	930.0	570.0	145.0	0.0
35	12.7	1.86	33.0	890.0	870.0	530.0	128.0	0.0
30	10.5	1.66	32.0	600.0	810.0	490.0	110.0	0.0
25	8.4	1.48	32.0	370.0	740.0	450.0	93.0	0.0

*Table 3: Main Engine Gas Mode Table of Capacities*

<b>Fuel Oil Mode (TIER III) ISO CONDITIONS</b>						
<b>Load</b>	<b>Power</b>	<b>Speed</b>	<b>SFOC</b>	<b>Exh.gas amount</b>	<b>Exh.gas temperature</b>	<b>Steam</b>
<b>%SMCR</b>	<b>kW</b>	<b>r/min</b>	<b>g/kWh</b>	<b>kg/s</b>	<b>°C</b>	<b>kg/h</b>
100	12590.0	69.0	161.5	26.2	232.0	1341.0
95	11961.0	67.8	160.3	25.3	225.0	1188.0
90	11331.0	66.6	159.4	24.3	219.0	1058.0
85	10702.0	65.4	158.6	23.3	211.0	869.0
80	10072.0	64.1	158.6	22.4	205.0	722.0
75	9443.0	62.7	158.8	21.3	204.0	684.0
70	8813.0	61.3	157.4	20.1	206.0	697.0
65	8184.0	59.8	156.5	18.9	210.0	729.0
60	7554.0	58.2	157.0	17.8	212.0	731.0
55	6925.0	56.5	157.6	16.6	213.0	719.0
50	6295.0	54.8	158.4	15.5	214.0	701.0
45	5666.0	52.9	159.6	14.1	221.0	753.0
40	5036.0	50.8	160.9	14.0	196.0	406.0
35	4407.0	48.6	162.4	12.8	202.0	450.0
30	3777.0	46.2	163.9	10.5	221.0	605.0
25	3148.0	43.5	165.6	8.3	234.0	634.0
20	2519.0	40.8	167.3	6.1	247.0	663.0
15	1890.0	38.1	169.0	3.9	260.0	692.0
10	1261.0	35.4	170.7	1.7	273.0	721.0

*Table 4: Main Engine Fuel Mode Performance Table*

For the purpose of the calculation of the tables above, we extracted data from the MAN CEAS Engine Data report of the engine.

The next tables contain data used for the calculations of the auxiliary engines performance. These data are taken from WÄRTSILÄ 34DF Product Guide for the 6L34DF and 8L34DF models respectively (*Wärtsilä 34DF Product Guide, 2017*).

**6L34DF Engine capacity data / rated power 480 kW per cylinder @ 720rpm (Gas Mode)**

Charge air		Lubricating oil		Cylinder jacket	
Heat dissipation (kW)	Low temperature cooling water flow (m <sup>3</sup> /h)	heat dissipation (kW)	Low temperature cooling water flow (m <sup>3</sup> /h)	heat dissipation (kW)	high temperature cooling water flow (m <sup>3</sup> /h)
494	60	278	60	359	60
Gas data					
Combustion air consumption (kg/h)	exhaust gas flow (kg/h)	exhaust gas temperature (°C)	allowable exhaust gas back pressure max (mbar)		
15480	15840	359	40		
Starting air			Pump capacities		
air consumption per start (N*m <sup>3</sup> )	Starting air source pressure <b>MAX</b> (bar)	Starting air source pressure <b>MIN</b> (bar)	lubricating oil pump 8 bar (m <sup>3</sup> /h)	High temperature cooling water pump (1 - 2.5 bar) (m <sup>3</sup> /h)	Low temperature cooling water pump (1 - 2.5 bar) (m <sup>3</sup> /h)
4.7	30	15	78	60	60

Table 5: 6L34DF Engine Capacity Data (Gas Mode)

6L34DF Engine performance (Gas Mode)									
Load %	Cylinder data		Combustion air data		Exhaust gas data		Heat balance data		
	Cylinder output (kW)	Mean effective pressure (bar)	Mass flow (kg/kWh)	Air temperature after cooler (°C)	Mass flow (kg/kWh)	Gas temperature after turbine (°C)	Charge air (kW)	Lubricating oil (kW)	Jacket cooling water (kW)
25	120	5.5	1.075	55	2	430	181.25	69.5	89.75
50	240	11	2.15	55	2.9	404	362.5	139	179.5
75	360	16.5	3.225	45	3.8	378	543.75	208.5	269.25
85	408	18.7	3.655	45	3.8	367.6	616.25	236.3	305.15
100	480	22	4.3	45	4.4	359	725	278	359
110	528	24.2	4.73	45	4.8	353.27	797.5	305.8	394.9

Table 6: 6L34DF Generator Performance Data (Gas Mode) (1)

6L34DF Engine performance (Gas Mode)		
Load %	SFGC (g/kWh)	SPOC (g/kWh)
25	183.9	5.2
50	170.0	3.9
75	156.0	2.6
85	151.7	2.3
100	148.9	1.9
110	147.0	1.6

Table 7: 6L34DF Generator Performance Data (Gas Mode) (2)

**6L34DF Engine capacity data / rated power 480 kW per cylinder @ 720rpm (Liquid Fuel Mode)**

Charge air		Lubricating oil		Cylinder jacket	
Heat dissipation (kW)	Low temperature cooling water flow (m <sup>3</sup> /h)	heat dissipation (kW)	Low temperature cooling water flow (m <sup>3</sup> /h)	heat dissipation (kW)	high temperature cooling water flow (m <sup>3</sup> /h)
845	60	272	60	414	60
Gas data					
Combustion air consumption (kg/h)	exhaust gas flow (kg/h)	exhaust gas temperature (°C)	allowable exhaust gas back pressure max (mbar)		
19800	20160	337	40		
Starting air			Pump capacities		
air consumption per start (N*m <sup>3</sup> )	Starting air source pressure <b>MAX</b> (bar)	Starting air source pressure <b>MIN</b> (bar)	lubricating oil pump 8 bar (m <sup>3</sup> /h)	High temperature cooling water pump (1 - 2.5 bar) (m <sup>3</sup> /h)	Low temperature cooling water pump (1 - 2.5 bar) (m <sup>3</sup> /h)
4.7	30	15	78	60	60

Table 8: 6L34DF Engine Capacity Data (Liquid Fuel Mode)

**6L34DF Engine performance (Liquid Fuel Mode)**

Load %	Cylinder data		Combustion air data		Exhaust gas data		Heat balance data		
	Cylinder output (kW)	Mean effective pressure (bar)	Mass flow (kg/kWh)	Air temperature after cooler (°C)	Mass flow (kg/kWh)	Gas temperature after turbine (°C)	Charge air (kW)	Lubricating oil (kW)	Jacket cooling water (kW)
25	120	5.5	1.375	50	1.9	339	277.25	70.5	103.5
50	240	11	2.75	50	3.2	333	554.5	141	207
75	360	16.5	4.125	50	4.5	327	831.75	211.5	310.5
85	408	18.7	4.675	50	5	324.6	942.65	239.7	351.9
100	480	22	5.5	50	5.6	337	1109	282	414
110	528	24.2	6.05	50	6	345.3	1219.9	310.2	455.4

Table 9: 6L34DF Generator Performance Data (Liquid Fuel Mode) (1)

6L34DF Engine performance (Liquid Fuel Mode)		
Load %	SFGC (g/kWh)	SPOC (g/kWh)
25	199.8	0.0
50	193.6	0.0
75	187.4	0.0
85	187.9	0.0
100	190.5	0.0
110	192.2	0.0

Table 10: 6L34DF Generator Performance Data (Liquid Fuel Mode) (2)

### 8L34DF Engine capacity data / rated power 480 kW per cylinder @ 720rpm (Gas Mode)

Charge air		Lubricating oil		Cylinder jacket	
Heat dissipation (kW)	Low temperature cooling water flow (m <sup>3</sup> /h)	heat dissipation (kW)	Low temperature cooling water flow (m <sup>3</sup> /h)	heat dissipation (kW)	high temperature cooling water flow (m <sup>3</sup> /h)
659	75	370	101	478	75
Gas data					
Combustion air consumption (kg/h)	exhaust gas flow (kg/h)	exhaust gas temperature (°C)	allowable exhaust gas back pressure max (mbar)		
20880	21240	359	40		
Starting air			Pump capacities		
air consumption per start (N*m <sup>3</sup> )	Starting air source pressure MAX (bar)	Starting air source pressure MIN (bar)	lubricating oil pump 8 bar (m <sup>3</sup> /h)	High temperature cooling water pump (1 - 2.5 bar) (m <sup>3</sup> /h)	Low temperature cooling water pump (1 - 2.5 bar) (m <sup>3</sup> /h)
5.7	30	15	101	75	75

Table 11: 8L34DF Engine Capacity Data (Gas Mode)

8L34DF Engine performance (Gas Mode)									
Load %	Cylinder data		Combustion air data		Exhaust gas data		Heat balance data		
	Cylinder output (kW)	Mean effective pressure (bar)	Mass flow (kg/kWh)	Air temperature after cooler (°C)	Mass flow (kg/kWh)	Gas temperature after turbine (°C)	Charge air (kW)	Lubricating oil (kW)	Jacket cooling water (kW)
25	120	5.5	1.45	55	2.5	430	252.75	92.5	119.5
50	240	11	2.9	55	3.8	404	505.5	185	239
75	360	16.5	4.35	45	5.1	378	758.25	277.5	358.5
85	408	18.7	4.93	45	5.4	367.6	859.35	314.5	406.3
100	480	22	5.8	45	5.9	359	1011	370	478
110	528	24.2	6.38	45	6.2	353.3	1112.1	407	525.8

Table 12: 8L34DF Generator Performance Data (Gas Mode) (1)

8L34DF Engine performance (Gas Mode)		
Load %	SFGC (g/kWh)	SPOC (g/kWh)
25	183.9	5.2
50	170.0	3.9
75	156.0	2.6
85	151.7	2.3
100	148.9	1.9
110	147.0	1.6

Table 13: 8L34DF Generator Performance Data (Gas Mode) (2)

**8L34DF Engine capacity data / rated power 480 kW per cylinder @ 720rpm (Liquid Fuel Mode)**

Charge air		Lubricating oil		Cylinder jacket	
Heat dissipation (kW)	Low temperature cooling water flow (m <sup>3</sup> /h)	heat dissipation (kW)	Low temperature cooling water flow (m <sup>3</sup> /h)	heat dissipation (kW)	high temperature cooling water flow (m <sup>3</sup> /h)
1127	75	376	101	552	75
Gas data					
Combustion air consumption (kg/h)	exhaust gas flow (kg/h)	exhaust gas temperature (°C)	allowable exhaust gas back pressure max (mbar)		
26280	27000	337	40		
Starting air			Pump capacities		
air consumption per start (N*m <sup>3</sup> )	Starting air source pressure <b>MAX</b> (bar)	Starting air source pressure <b>MIN</b> (bar)	lubricating oil pump 8 bar (m <sup>3</sup> /h)	High temperature cooling water pump (1 - 2.5 bar) (m <sup>3</sup> /h)	Low temperature cooling water pump (1 - 2.5 bar) (m <sup>3</sup> /h)
5.7	30	15	101	75	75

*Table 14: 8L34DF Engine Capacity Data (Liquid Fuel Mode)*

**8L34DF Engine performance (Liquid Fuel Mode)**

Load %	Cylinder data		Combustion air data		Exhaust gas data		Heat balance data		
	Cylinder output (kW)	Mean effective pressure (bar)	Mass flow (kg/kWh)	Air temperature after cooler (°C)	Mass flow (kg/kWh)	Gas temperature after turbine (°C)	Charge air (kW)	Lubricating oil (kW)	Jacket cooling water (kW)
25	120	5.5	1.825	50	2.4	339	369.75	94	138
50	240	11	3.65	50	4.2	333	739.5	188	276
75	360	16.5	5.475	50	6	327	1109.25	282	414
85	408	18.7	6.205	50	6.6	324.6	1257.15	319.6	469.2
100	480	22	7.3	50	7.5	337	1479	376	552
110	528	24.2	8.03	50	8.1	345.3	1626.9	413.6	607.2

*Table 15: 8L34DF Generator Performance Data (Liquid Fuel Mode) (1)*

8L34DF Engine performance (Liquid Fuel Mode)		
Load %	SFGC (g/kWh)	SPOC (g/kWh)
25	199.8	0.0
50	193.6	0.0
75	187.4	0.0
85	187.9	0.0
100	190.5	0.0
110	192.2	0.0

Table 16: 8L34DF Generator Performance Data (Liquid Fuel Mode) (2)

With these data acquired from each engine's manual it is now possible to build the performance tables that GPROMS needs.

Performance Table																					
Load	"Speed"	"BSFC LFM"	"BSFC GFM"	"BSFC PLT"	MFLair GFM	"Texh GFM"	"TaC GFM"	"Tscav GFM"	"Pscav GFM"	"Qcac GFM"	"Qjct GFM"	"Qlub GFM"	MFLair LFM	"Texh LFM"	"TaC LFM"	"Tscav LFM"	"Pscav LFM"	"Qcac LFM"	"Qjct LFM"	"Qlub LFM"	
%	rpm	g/kWh	g/kWh	g/kWh	kg/s	K	K	K	Pa	W	W	W	kg/s	K	K	K	Pa	W	W	W	
1	1	1.1500	169.575	141.540	2.8035	25.3	495.15	481.04	310.15	415000	4410000	1680000	1020000	25.6352	505.15	481.04	310.15	415000	4410000	1680000	1020000
2	0.95	1.1300	168.315	140.385	2.8980	24.5	488.15	474.02	309.15	399000	4120000	1620000	980000	24.7674	498.15	474.02	309.15	399000	4120000	1620000	980000
3	0.9	1.1100	167.370	139.440	3.0030	23.7	483.15	468.58	308.15	382000	3830000	1550000	940000	23.7983	492.15	468.58	308.15	382000	3830000	1550000	940000
4	0.85	1.0900	166.530	138.705	3.1290	22.8	479.15	457.65	307.15	362000	3500000	1490000	900000	22.8285	484.15	457.65	307.15	362000	3500000	1490000	900000
5	0.8	1.0683	166.530	138.600	3.2550	21.8	477.15	450.96	306.15	347000	3220000	1430000	860000	21.9563	478.15	450.96	306.15	347000	3220000	1430000	860000
6	0.75	1.0450	168.328	139.920	3.4344	21.0	475.15	444.74	305.15	335000	2990000	1370000	820000	20.8835	477.15	444.74	305.15	335000	2990000	1370000	820000
7	0.7	1.0217	168.844	138.542	3.5934	19.8	476.15	434.37	304.15	312000	2830000	1310000	780000	19.7147	479.15	434.37	304.15	312000	2830000	1310000	780000
8	0.65	0.9967	165.890	137.598	3.7736	18.6	477.15	423.33	303.15	289000	2290000	1240000	750000	18.5442	483.15	423.33	303.15	289000	2290000	1240000	750000
9	0.6	0.9700	167.990	139.100	4.0125	17.5	479.15	414.07	303.15	269000	1980000	1180000	710000	17.4708	485.15	414.07	303.15	269000	1980000	1180000	710000
10	0.55	0.9417	168.632	139.421	4.2586	16.4	478.15	403.78	302.15	247000	1700000	1120000	680000	16.2968	486.15	403.78	302.15	247000	1700000	1120000	680000
11	0.5	0.9133	169.488	139.956	4.5388	15.3	479.15	392.14	301.15	228000	1420000	1060000	640000	15.2220	487.15	392.14	301.15	228000	1420000	1060000	640000
12	0.45	0.8817	172.368	142.020	4.9140	14.0	486.15	381.38	300.15	209000	1160000	990000	600000	13.8488	494.15	381.38	300.15	209000	1160000	990000	600000
13	0.4	0.8467	173.772	142.992	5.3136	14.1	459.15	377.72	299.15	202000	1130000	900000	570000	13.7749	469.15	377.72	299.15	202000	1130000	900000	570000
14	0.35	0.8100	175.392	143.866	5.7996	12.7	461.15	374.85	306.15	186000	890000	670000	530000	12.6012	475.15	374.85	306.15	186000	890000	670000	530000
15	0.3	0.7700	177.012	144.720	6.4368	10.5	480.15	361.17	305.15	166000	600000	610000	490000	10.3280	484.15	361.17	305.15	166000	600000	610000	490000
16	0.25	0.7250	178.848	145.584	7.2684	8.4	493.15	348.33	305.15	148000	370000	740000	450000	8.1562	507.15	348.33	305.15	148000	370000	740000	450000
17	0.2	0.6800	180.684	146.448	8.1000	6.3	506.15	335.50	305.15	130000	140000	670000	410000	5.9829	520.15	335.50	305.15	130000	140000	670000	410000
18	0.15	0.6350	182.520	147.312	8.9316	4.2	519.15	322.66	305.15	112000	0	600000	370000	3.8113	533.15	322.66	305.15	112000	0	600000	370000
19	0.1	0.5900	184.356	148.176	9.7632	4.2	519.15	309.82	305.15	94000	0	530000	330000	3.8113	533.15	309.82	305.15	94000	0	530000	330000
20	0.05	0.5450	186.192	149.040	10.5948	4.2	519.15	296.98	305.15	76000	0	460000	290000	3.8113	533.15	296.98	305.15	76000	0	460000	290000
21	0.00001	0.5000	188.028	149.904	11.4264	4.2	519.15	284.14	305.15	0	0	390001	250001	3.8113	533.15	284.14	305.15	0	0	390001	250001

Table 17: 5G70ME-C10-G1 2-stroke Engine Performance Table

Performance Table																					
Load	"Speed"	"BSFC LFM"	"BSFC GFM"	"BSFC PLT"	MFLair GFM	"Texh GFM"	"TaC GFM"	"Tscav GFM"	"Pscav GFM"	"Qcac GFM"	"Qjct GFM"	"Qlub GFM"	MFLair LFM	"Texh LFM"	"TaC LFM"	"Tscav LFM"	"Pscav LFM"	"Qcac LFM"	"Qjct LFM"	"Qlub LFM"	
	rpm				kg/s	K	K	K	Pa	W	W	W	kg/s	K	K	K	Pa	W	W	W	
1	1.10	12	201.85	154.35	1.6	4.1624	626.42	335.57	318.15	242000	797500	394900	305800	5.3240	618.42	343.98	323.15	2420000	1219900	455400	310200
2	1.00	12	200.03	156.31	1.9	3.4400	632.15	337.31	318.15	220000	725000	359000	278000	4.4000	610.15	346.06	323.15	2200000	1109000	414000	282000
3	0.85	12	197.30	159.26	2.3	2.4854	640.75	340.69	318.15	187000	616250	305150	236300	3.1790	597.75	350.11	323.15	1870000	942650	351900	239700
4	0.75	12	198.64	165.41	2.6	1.9350	651.15	343.70	318.15	165000	543750	269250	208500	2.4750	600.15	353.70	323.15	1650000	831750	310500	211500
5	0.50	12	207.15	181.89	3.9	0.8600	677.15	366.47	328.15	110000	362500	179500	139000	1.1000	606.15	368.98	323.15	1100000	554500	207000	141000
6	0.25	12	215.78	198.65	5.2	0.2150	703.15	404.79	328.15	55000	181250	89750	69500	0.2750	612.15	414.80	323.15	550000	277250	103500	70500
7	0.10	12	220.96	208.71	5.98	0.22	718.75	358.81	328.15	22000	72500	35900	27800	0.2750	615.75	442.30	323.15	220000	110900	41400	28200
8	0.00	12	224.42	215.41	6.50	0.22	729.15	358.81	328.15	22000	72500	35900	27800	0.2750	618.15	460.63	323.15	220000	110900	41400	28200

Table 18: 6L34DF Auxiliary Engine Performance Table

Performance Table																					
Load	"Speed"	"BSFC LFM"	"BSFC GFM"	"BSFC PLT"	MFLair GFM	"Texh GFM"	"TaC GFM"	"Tscav GFM"	"Pscav GFM"	"Qcac GFM"	"Qjct GFM"	"Qlub GFM"	MFLair LFM	"Texh LFM"	"TaC LFM"	"Tscav LFM"	"Pscav LFM"	"Qcac LFM"	"Qjct LFM"	"Qlub LFM"	
	rpm				kg/s	K	K	K	Pa	W	W	W	kg/s	K	K	K	Pa	W	W	W	
1	1.10	12	201.85	154.35	1.6	7.4859	626.42	331.66	318.15	242000	1112100	525800	407000	9.4219	618.42	338.85	323.15	2420000	1626900	607200	413600
2	1.00	12	200.03	156.31	1.9	6.1867	632.15	333.01	318.15	220000	1011000	478000	370000	7.7867	610.15	340.42	323.15	2200000	1479000	552000	376000
3	0.85	12	197.30	159.26	2.3	4.4699	640.75	335.63	318.15	187000	859350	406300	314500	5.6259	597.75	343.46	323.15	1870000	1257150	469200	319600
4	0.75	12	198.64	165.41	2.6	3.4800	651.15	337.96	318.15	165000	758250	358500	277500	4.3800	600.15	346.17	323.15	1650000	1109250	414000	282000
5	0.50	12	207.15	181.89	3.9	1.5467	677.15	357.86	328.15	110000	505500	239000	185000	1.9467	606.15	357.68	323.15	1100000	739500	276000	188000
6	0.25	12	215.78	198.65	5.2	0.3867	703.15	387.57	328.15	55000	252750	119500	92500	0.4867	612.15	392.22	323.15	550000	369750	138000	94000
7	0.10	12	220.96	208.71	5.98	0.39	718.75	351.92	328.15	22000	101100	47800	37000	0.4867	615.75	412.94	323.15	220000	147900	55200	37600
8	0.00	12	224.42	215.41	6.50	0.39	729.15	351.92	328.15	22000	101100	47800	37000	0.4867	618.15	426.75	323.15	220000	147900	55200	37600

Table 19: 8L34DF Auxiliary Engine Performance Table

Following the integration of the performance tables into the model, the next crucial step involves preparing and refining the corresponding code to enable accurate simulation and generation of the desired results. This process begins by identifying the key parameters that the program should calculate, based on the objectives of the study. Once these parameters are defined, they are implemented in the code through appropriate mathematical formulations and logical structures. Subsequently, thorough debugging is carried out to ensure the accuracy and stability of the model, eliminating any inconsistencies or computational errors. By carefully structuring the code, it becomes possible to replicate realistic operating scenarios and extract meaningful performance indicators, which are essential for the comparative analysis carried out in the context of this study.

The model based assessment of the conventional LNGC will be conducted twice. Once with Shaft Generators (PTO) and once without. By default, the presence of a Power Take-Off (PTO) system improves the overall performance of the vessel. Shaft generators, powered by the main engine, are used to supply electrical power to the ship's main systems. These generators must maintain a stable voltage and frequency output, even as the main engine's speed varies. The main advantages of incorporating a PTO include lower fuel consumption, decreased carbon emissions, reduced maintenance expenses, and diminished noise levels (*Wärtsilä Shaft Generators*, n.d.). The results matrix is then produced in the GPROMS language with the following parameters that will be explained later.

```
ResultsNames := ["Mode_index", "Vspeed", "Draft", "Prop_Demand", "NBOG", "ME_Load_001%", "ME_Load_002%", "DG_Load_6L_001%", "DG_Load_6L_004%",
"DG_Load_8L_002%", "DG_Load_8L_003%", "P_el_tot", "Cargo_Consumption_per_day", "GCU_Consumption_per_day",
"Pilot_Fuel_Consumption_per_day", "Energy_LNG_per_day", "Energy_pilot_per_day", "Energy_total_per_day", "eff_ME_001",
"eff_ME_002", "eff_DG_6L_001", "eff_DG_6L_004", "eff_DG_8L_002", "eff_DG_8L_003", "r_cargo_consumed", "r_hotel",
"r_propulsion", "r_parasitic", "r_GCU", "r_pto", "eff_system", "eff_Ship"] ;
```

Figure 12: Results Names for Conventional LNGC Model

```
1018 Results("Vspeed") = Operational_Model_Modes.Vs ;
1019 Results("Draft") = Operational_Model_Modes.Td ;
1020 Results("Prop_Demand") = (PropellerCurve001.Fd+PropellerCurve002.Fd)/1000 ;
1021 Results("NBOG") = Source_TankBOG.out_mass_flowrate/1000*60*60*24 ;
1022 Results("ME_Load_001%") = M_5G70MEGI_C10_001.Load*100 ;
1023 Results("ME_Load_002%") = M_5G70MEGI_C10_002.Load*100 ;
1024 Results("DG_Load_6L_001%") = W_6L34DF_001.Load*100 ;
1025 Results("DG_Load_6L_004%") = W_6L34DF_004.Load*100 ;
1026 Results("DG_Load_8L_002%") = W_8L34DF_002.Load*100 ;
1027 Results("DG_Load_8L_003%") = W_8L34DF_003.Load*100 ;
1028 Results("P_el_tot") = (measEL_Hotel.measurement.signal+measEL_LDComp.measurement.signal+measEL_RLQ.measurement.signal)/1000 ;
1029 Results("Cargo_Consumption_per_day") = (FGHS_GasManagement.FBOG+Source_TankBOG.out_mass_flowrate-LNG_to_TankReturn.in_mass_flowrate)/1000*60*60*24 ;
1030 Results("GCU_Consumption_per_day") = measGCU_Mflow.measurement.signal/1000*60*60*24 ;
1031 Results("Pilot_Fuel_Consumption_per_day") = (M_5G70MEGI_C10_001.mflow_pilot+M_5G70MEGI_C10_002.mflow_pilot+W_6L34DF_001.mflow_pilot+W_6L34DF_004.mflow_pilot+W_8L34DF_002.mflow_pilot+W_8L34DF_003.mflow_pilot)/1000*60*60*24 ;
1032 Results("Energy_LNG_per_day") = (FGHS_GasManagement.FBOG+meas_LHV_FBOG.LHV+Source_TankBOG.out_mass_flowrate*meas_LHV_NBOG.LHV-LNG_to_TankReturn.in_mass_flowrate*meas_LHV_returnLNG.LHV)/1000*60*60*24 ;
1033 Results("Energy_pilot_per_day") = (M_5G70MEGI_C10_001.mflow_pilot+W_6L34DF_001.mflow_pilot+W_8L34DF_003.mflow_pilot+M_5G70MEGI_C10_002.mflow_pilot+W_6L34DF_004.mflow_pilot+W_8L34DF_002.mflow_pilot)*M_5G70MEGI_C10_001.LHVact_liq/1000*60*60*24 ;
1034 Results("Energy_total_per_day") = Results("Energy_LNG_per_day")+Results("Energy_pilot_per_day") ;
1035 Results("eff_ME_001") = M_5G70MEGI_C10_001.Load*12590000/(M_5G70MEGI_C10_001.mflow_fuel*M_5G70MEGI_C10_001.LHVact_gas+M_5G70MEGI_C10_001.mflow_pilot*M_5G70MEGI_C10_001.LHVact_liq) ;
1036 Results("eff_ME_002") = M_5G70MEGI_C10_002.Load*12590000/(M_5G70MEGI_C10_002.mflow_fuel*M_5G70MEGI_C10_002.LHVact_gas+M_5G70MEGI_C10_002.mflow_pilot*M_5G70MEGI_C10_002.LHVact_liq) ;
1037 Results("eff_DG_6L_001") = W_6L34DF_001.Load*2880000/(W_6L34DF_001.mflow_fuel*W_6L34DF_004.LHVact_gas+W_6L34DF_001.mflow_pilot*W_6L34DF_004.LHVact_liq) ;
1038 Results("eff_DG_6L_004") = W_6L34DF_004.Load*2880000/(W_6L34DF_001.mflow_fuel*W_6L34DF_004.LHVact_gas+W_6L34DF_001.mflow_pilot*W_6L34DF_004.LHVact_liq) ;
1039 Results("eff_DG_8L_002") = W_8L34DF_002.Load*3840000/(W_8L34DF_002.mflow_fuel*W_8L34DF_003.LHVact_gas+W_8L34DF_002.mflow_pilot*W_8L34DF_003.LHVact_liq) ;
1040 Results("eff_DG_8L_003") = W_8L34DF_003.Load*3840000/(W_8L34DF_002.mflow_fuel*W_8L34DF_003.LHVact_gas+W_8L34DF_002.mflow_pilot*W_8L34DF_003.LHVact_liq) ;
1041 Results("r_cargo_consumed") = Results("Cargo_Consumption_per_day")/(Source_TankBOG.out_mass_flowrate/1000*60*60*24) ;
1042 Results("r_hotel") = measEL_Hotel.measurement.signal/Results("P_el_tot")/1000 ;
1043 Results("r_propulsion") = Results("Prop_Demand")/Results("P_el_tot") ;
1044 Results("r_parasitic") = (measEL_RLQ.measurement.signal+measEL_LDComp.measurement.signal)/Results("P_el_tot")/1000 ;
1045 Results("r_GCU") = Results("GCU_Consumption_per_day")/(Source_TankBOG.out_mass_flowrate/1000*60*60*24) ;
1046 Results("r_pto") = -(measEL_PTO_001.measurement.signal+measEL_PTO_002.measurement.signal)/Results("P_el_tot")/1000 ;
1047 Results("eff_system") = (Results("Prop_Demand")+1000+measEL_Hotel.Power_meas+measEL_RLQ.measurement.signal)/(M_5G70MEGI_C10_001.HeatInput+M_5G70MEGI_C10_002.HeatInput+W_6L34DF_001.HeatInput+W_8L34DF_002.HeatInput+W_8L34DF_003.HeatInput+W_6L34DF_004.HeatInput) ;
1048 Results("eff_Ship") = (Results("Prop_Demand")+measEL_Hotel.Power_meas/1000)*60*60*24/Results("Energy_total_per_day") ;
```

Figure 13: Coding of the "Results" Table in GPROMS Language for Conventional LNGC Model

## COGES System

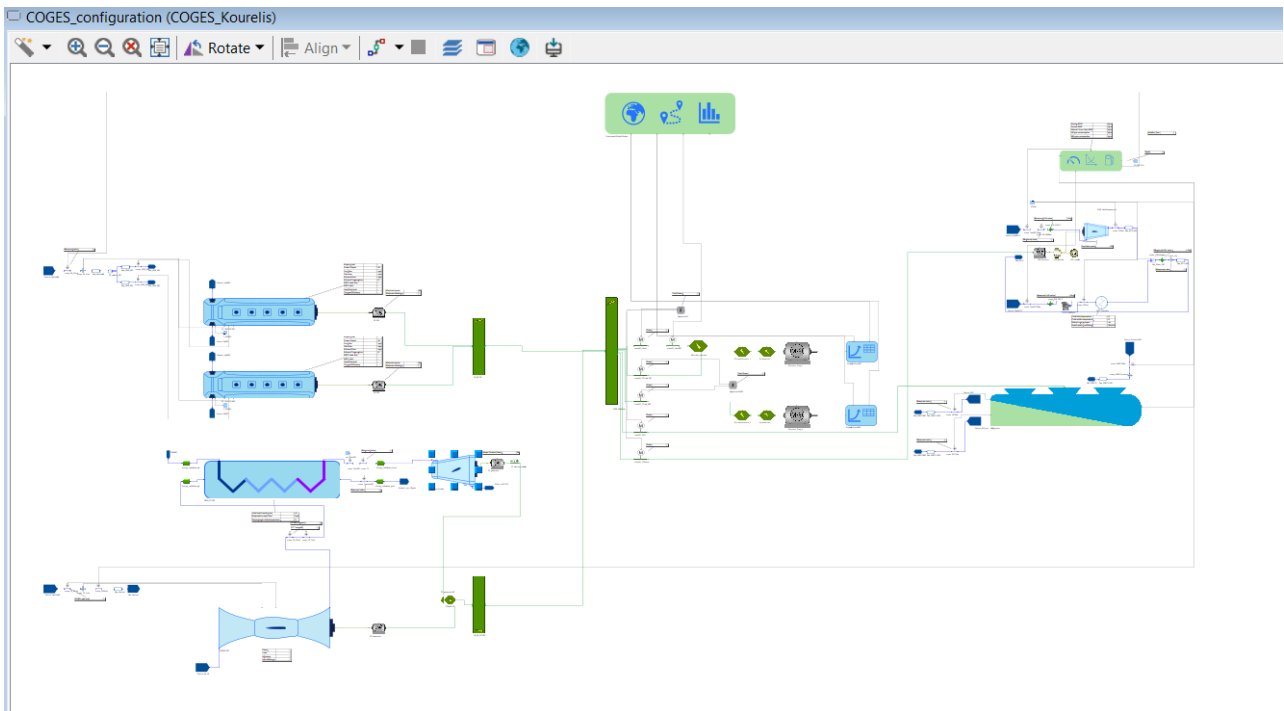


Figure 14: COGES System Propulsion Model in GPROMS Interface

The development of the COGES model in GPROMS requires the integration of specific technical data that define the behavior and performance of each subsystem. In particular, the necessary inputs include the operational and performance characteristics of the two Wärtsilä 10V31SG generators (*Wärtsilä 31SG*, 2025), which are used as the gas engines in the reference configuration. Additionally, detailed technical specifications and performance maps for both the SGT400 gas turbine (*SGT-400 Gas Turbine*, 2025) and the heat recovery steam generator (HRSG) are essential for accurately modeling the thermodynamic interactions within the combined cycle system. All of these data sets were provided directly by the university and originated from an internal database developed at NTUA, meaning that no additional data collection or external research was required. These inputs form the foundation of the COGES model and ensure a realistic representation of its operation under various load conditions, allowing for a robust and consistent comparison with traditional propulsion technologies.

HRSG_COGES (HX_OTPHEVSH_simple)			
General	<input checked="" type="checkbox"/>	Total heat transfer area	6303 m <sup>2</sup>
Shell side HT	<input type="checkbox"/>	Evaporation mass flow	4.9 kg/s
Tube side HT	<input type="checkbox"/>	Tst_outlet	525 °C
Initialisation	<input checked="" type="checkbox"/>	Superheater delta temperature	25 K

Figure 15: Data Input for HRSG System

W\_10V31SG\_001 (RecipEngine\_4)

**General**

**Performance**

**Fuels**

- Fuel Mode Gas Fuel ▾
- Gas Fuel Composition Controlled ▾
- Nominal Power Output 5300 kW ▾
- Power Output 4680 kW ▾
- Engine Load 1
- Engine speed 12 rps
- Ambient correction method None ▾
- Reference Air ambient temperature 298.15 K ▾
- Reference Sea ambient temperature 298.15 K ▾

Figure 16: Data Input for W10V31SG

SGT400\_001 (GasTurbine\_simple\_2)

**Nominal point**

**General**

**Performance**

**Fuel**

**Initialisation**

- Tamb performance Num of Data 8
- Max Performance wrt Tamb

		DimTPerf				
		Tamb	Power_max	eff_max	mgas_max	Tgas_max
Tamb performance Num of Data	1	273.15	1.1566	1.0395	1.1086	0.9777
	2	278.15	1.0976	1.0268	1.0696	0.9846
	3	283.15	1.0495	1.0130	1.0342	0.9927
	4	288.15	1.0000	1.0000	1.0000	1.0000
	5	293.15	0.9523	0.9859	0.9665	1.0077
	6	298.15	0.9080	0.9717	0.9348	1.0156
	7	303.15	0.8664	0.9568	0.9041	1.0239
	8	308.15	0.8255	0.9405	0.8733	1.0329

- Tamb\_LB 223 K ▾
- Tamb\_UB 323 K ▾
- Part load performance Num of Data 10
- Performance wrt Load

		DimPLperf			
		Load	Reff	Rmgas	RTgas
Part Load performance Num of Data	1	1	1.002551	0.999588	1
	2	0.9	0.974629	0.960681	0.990919
	3	0.8	0.933414	0.920272	0.998527
	4	0.7	0.878904	0.87836	1.00479
	5	0.6	0.8111	0.834946	1.011539
	6	0.5	0.730002	0.790028	1.01645
	7	0.4	0.635609	0.743609	1.021257
	8	0.3	0.527922	0.695687	1.025274
	9	0.2	0.406941	0.646262	1.028613
	10	0	0.406941	0.646262	1.028613

- load\_LB 0.0
- load\_UB 1.0

Figure 17: Data Input for SGT400

Figure 18: Data Input for Steam Turbine

The same procedure as in the conventional LNGC carrier has been practiced in the COGES model in GPROMS and the following variables have been derived.

```

225 ResultsNames := ["Mode_index", "Vspeed", "Draft", "Prop_Demand", "NBOG", "SGT400_Load_%", "DG_Load_01_%", "DG_Load_02_%", "P_GT_el", "P_ST_el",
226 "P_el_tot", "Cargo_Consumption_per_day", "GCU_Consumption_per_day", "Energy_Total_per_day", "eff_SGT400", "eff_COGES",
227 "eff_DG_1", "eff_DG_2", "r_cargo_consumed", "r_hotel", "r_propulsion", "r_GT", "r_parasitic", "r_GCU", "eff_PT_el",
228 "eff_system", "eff_ship"];

```

Figure 19: Results Names for COGES System Model

```

COGES_configuration (COGES_Kourelis)
398 HVSB_shipmain.Power_active_in(1) = MLN(HVSB_shipmain.Power_active_tot-100, PCOGES_high);
399 END
400
401 eff_totCC = HV_SB_COGES.Power_active_tot / (SGT400_001.mflow_fuel * SGT400_001.LHV_fuel);
402 # /// COGES module - Model Equations /// END
403
404 Results("Mode_index") = Operational_Model_Modes.xMode ;
405 Results("Vspeed") = Operational_Model_Modes.Vs ;
406 Results("Draft") = Operational_Model_Modes.Td ;
407 Results("Prop_Demand") = (PropellerCurve001.Pd+PropellerCurve002.Pd)/1000 ;
408 Results("NBOG") = FGHS_GasManagement.NBOG/1000*60*60*24 ;
409 Results("SGT400_Load_%") = SGT400_001.load*100 ;
410 Results("DG_Load_01_%") = W_10V31SG_001.Load*100 ;
411 Results("DG_Load_02_%") = W_10V31SG_002.Load*100 ;
412 Results("P_GT_el") = GT_generator.Power_electrical ;
413 Results("P_ST_el") = ST_generator.Power_electrical ;
414 Results("P_el_tot") = (measEL_Hotel.measurement.signal+measEL_LDComp.measurement.signal+measEL_RLQ.measurement.signal+
415 measEL_PTtrain_001.measurement.signal+measEL_PTtrain_002.measurement.signal)/1000 ;
416 Results("Cargo_Consumption_per_day") = (FGHS_GasManagement.FBOG+FGHS_GasManagement.NBOG-meas_RLQflow.measurement.signal)/1000*60*60*24 ;
417 Results("GCU_Consumption_per_day") = meas_GCUflow.measurement.signal/1000*60*60*24 ;
418 Results("Energy_Total_per_day") = (FGHS_GasManagement.Gas_demandME.signal+FGHS_GasManagement.Gas_demandAE.signal)*meas_LHVtoEngines.LHV/1000*60*60*24 ;
419 Results("eff_SGT400") = SGT400_001.eff ;
420 Results("eff_COGES") = eff_totCC ;
421 Results("eff_DG_1") = W_10V31SG_001.Load*5300000/(W_10V31SG_001.mflow_fuel*W_10V31SG_001.LHVact_gas) ;
422 Results("eff_DG_2") = W_10V31SG_002.Load*5300000/(W_10V31SG_002.mflow_fuel*W_10V31SG_002.LHVact_gas) ;
423 Results("r_cargo_consumed") = Results("Cargo_Consumption_per_day")*1000/(FGHS_GasManagement.NBOG*60*60*24) ;
424 Results("r_hotel") = measEL_Hotel.measurement.signal/Results("P_el_tot")/1000 ;
425 Results("r_propulsion") = Results("Prop_Demand")/Results("P_el_tot") ;
426 Results("r_GT") = Results("P_ST_el")/Results("P_el_tot") ;
427 Results("r_parasitic") = (measEL_RLQ.measurement.signal+measEL_LDComp.measurement.signal)/Results("P_el_tot")/1000 ;
428 Results("r_GCU") = Results("GCU_Consumption_per_day")/(FGHS_GasManagement.NBOG/1000*60*60*24) ;
429 Results("eff_PT_el") = Results("Prop_Demand")/(measEL_PTtrain_001.measurement.signal+measEL_PTtrain_002.measurement.signal)*1000 ;
430 Results("eff_system") = (Results("Prop_Demand")+1000*measEL_Hotel.Power_meas+measEL_RLQ.measurement.signal)/(W_10V31SG_001.HeatInput+W_10V31SG_002.HeatInput+
431 FGHS_GasManagement.Gas_demandME.signal*meas_LHVtoEngines.measurement.signal) ;
432 Results("eff_ship") = (Results("Prop_Demand")+measEL_Hotel.Power_meas/1000)*60*60*24/Results("Energy_total_per_day") ;
433
434

```

Figure 20: Coding of the "Results" Table in GPROMS Language for COGES System Model

## Analysis of Results Table

The results that the two models produce and are to be considered in the comparison are the following:

- Vessel Speed [kn]
- Draft [m]
- Propulsion Demand [kW]
- Natural Boil-off Gas [t/day]
- Main Engine Load [kW]
- Generator Load [kW]
- Gas Turbine Load [kW]
- Total Electric Power [kW]
- Daily Cargo Consumption [t/day]
- Daily GCU Consumption [t/day]
- Daily Pilot Fuel Consumption [t/day]
- Daily Energy Consumption by LNG [kW/day]
- Daily Energy Consumption by Pilot Fuel [kW/day]
- Daily Energy Consumption Total [kW/day]
- Main Engine Efficiency
- Generator Efficiency
- Gas Turbine Efficiency

On top of these one must also measure the value of a few numerical coefficients that help understand the comparison better. Each coefficient is symbolized with the letter r and the description of each one:

- $r_{\text{cargo\_consumed}}$ : LNG consumed in relation to the boil off gas evaporated naturally.
- $r_{\text{hotel}}$ : Ship's hotel energy consumption compared to total energy produced
- $r_{\text{GCU}}$ : The percentage of the boil-off gas that is burned in the GCU
- $r_{\text{propulsion}}$ : The propulsion demand compared to the total electrical power
- $r_{\text{parasitic}}$ : The reliquifaction system and compressors electricity demand (parasitic) compared to the total electrical power

Finally, there are three additional indexes that describe the efficiency of other significant parts of the vessel and are analyzed in the following formulas:

- $$n_{PTel} = \frac{\text{Propulsion Demand}}{\text{Power Delivered to Propellers}}$$
- $$n_{System} = \frac{\text{Propulsion Demand} + \text{Power Consumed RLQ} + \text{Power Consumed Hotel}}{\text{Engines Heat Input}}$$
- $$n_{Ship} = \frac{\text{Propulsion Demand} + \text{Power Consumed Hotel}}{\text{Energy Consumption}}$$

# Simulation Results

## Initial Test

The initial test contains the analysis of the three following models:

1. Conventional LNGC without Shaft Generators
2. Conventional LNGC with Shaft Generators
3. LNGC with COGES System

GPROMS Model Builder produces the desired results in relation to the vessel's speed. It is important to note that the program also composes these four non-sailing points:

1. Anchorage Ballast
2. Loading
3. Anchorage Laden
4. Discharging

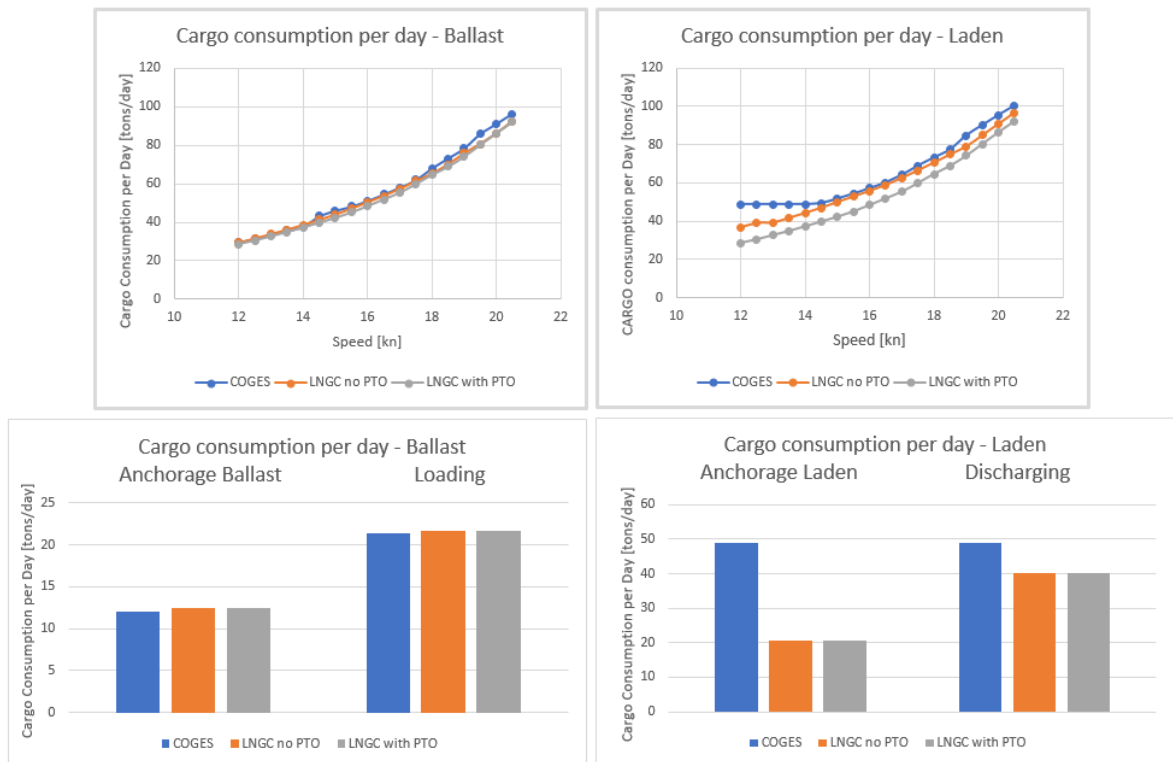


Figure 21: Cargo Consumption per Day

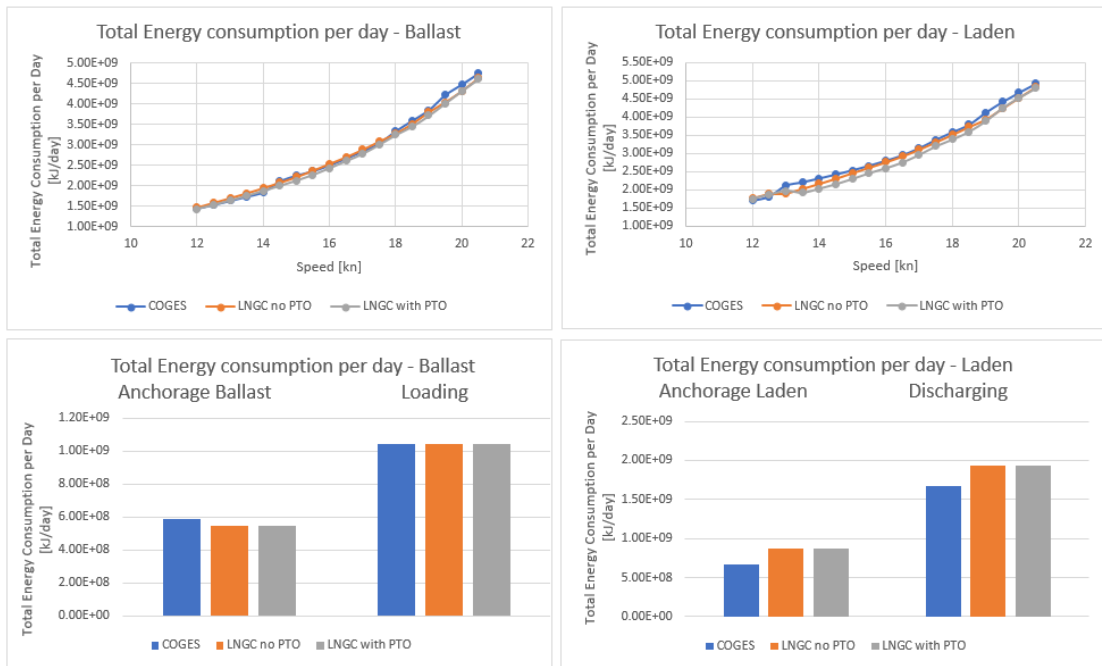


Figure 22: Total Energy Consumption per Day

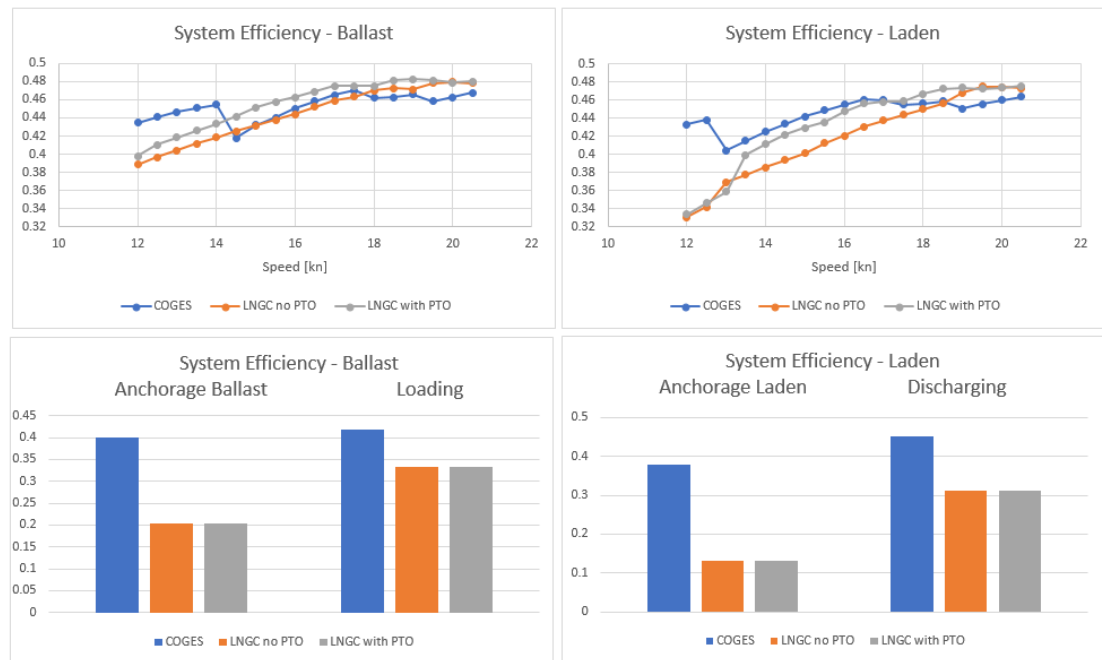


Figure 23: System Efficiency

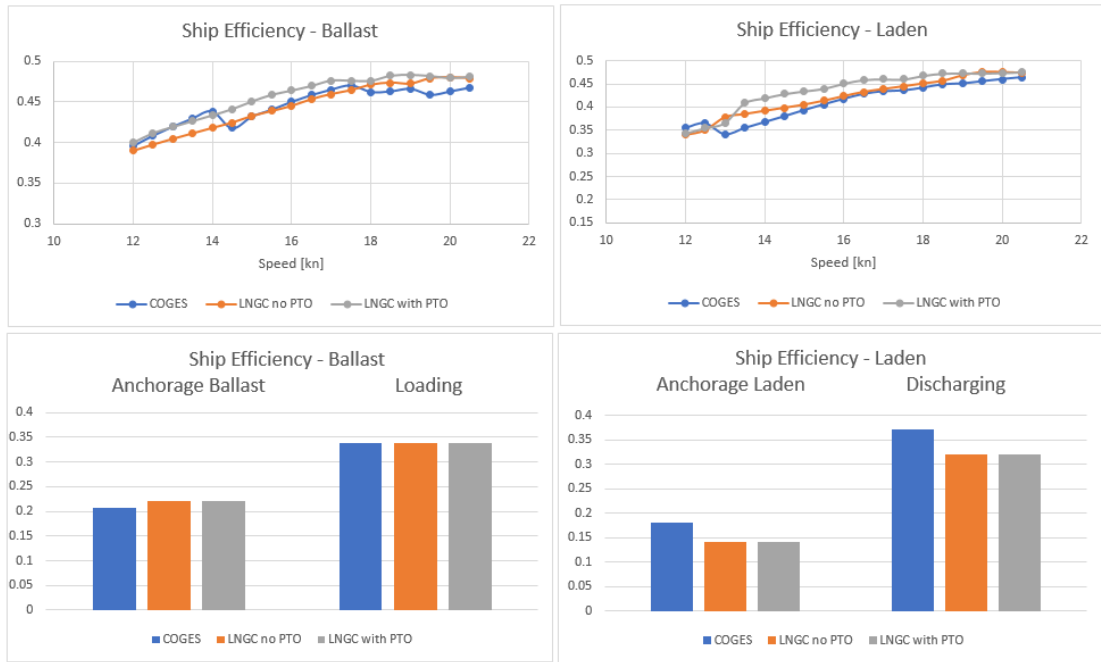


Figure 24: Ship Efficiency

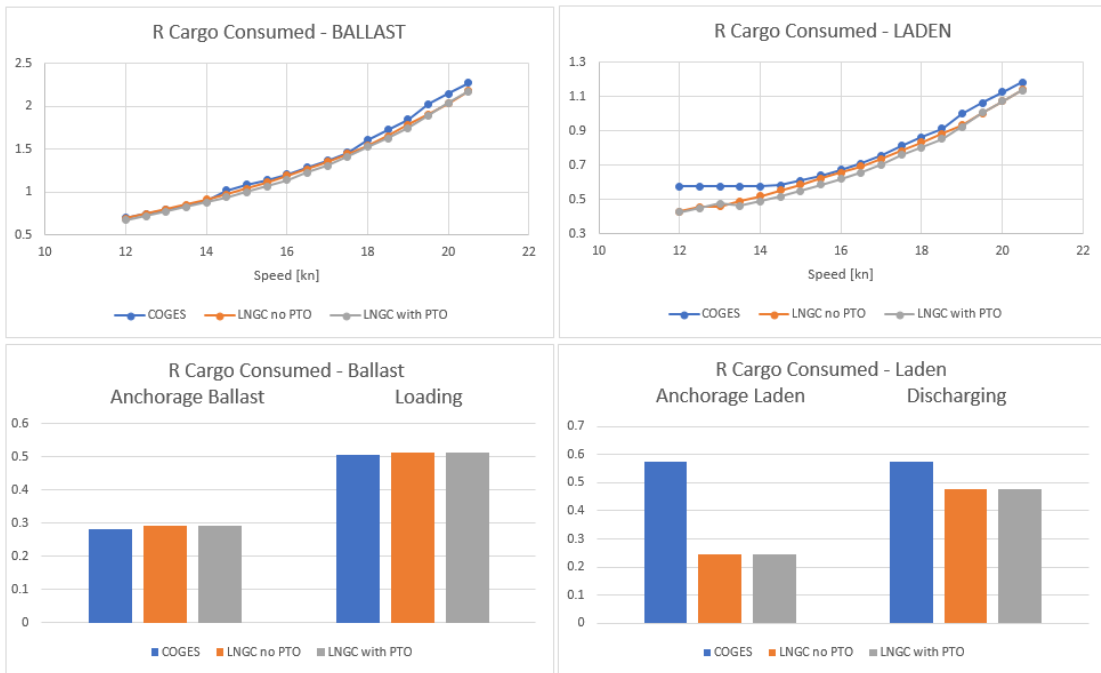


Figure 25: R Cargo Consumed

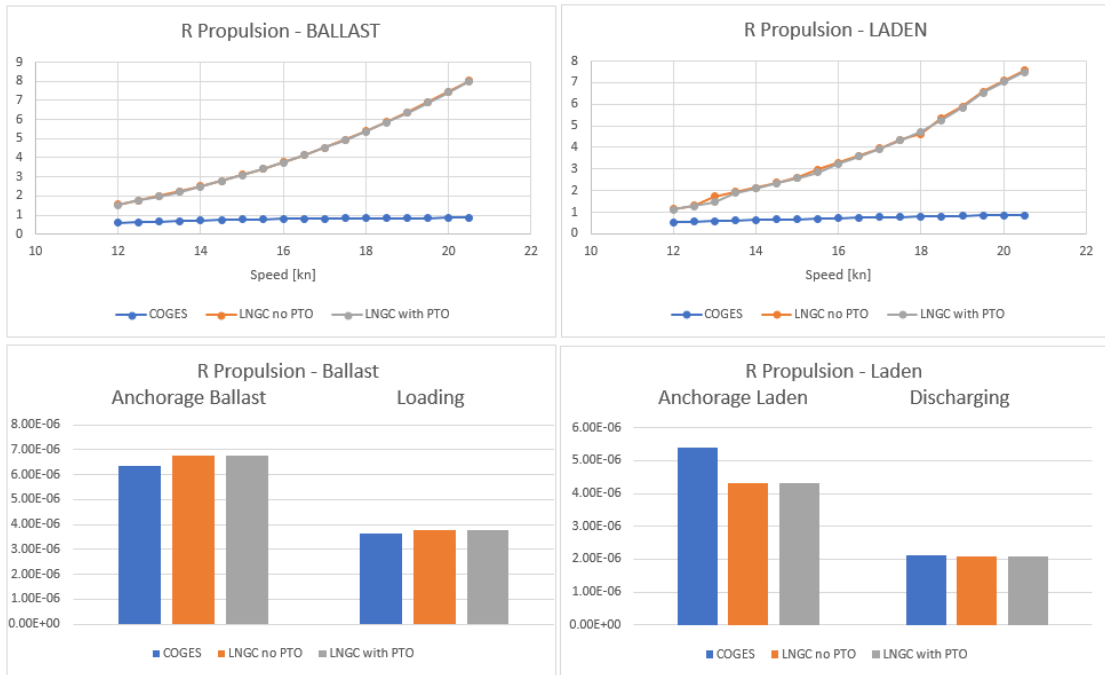


Figure 26: R Propulsion

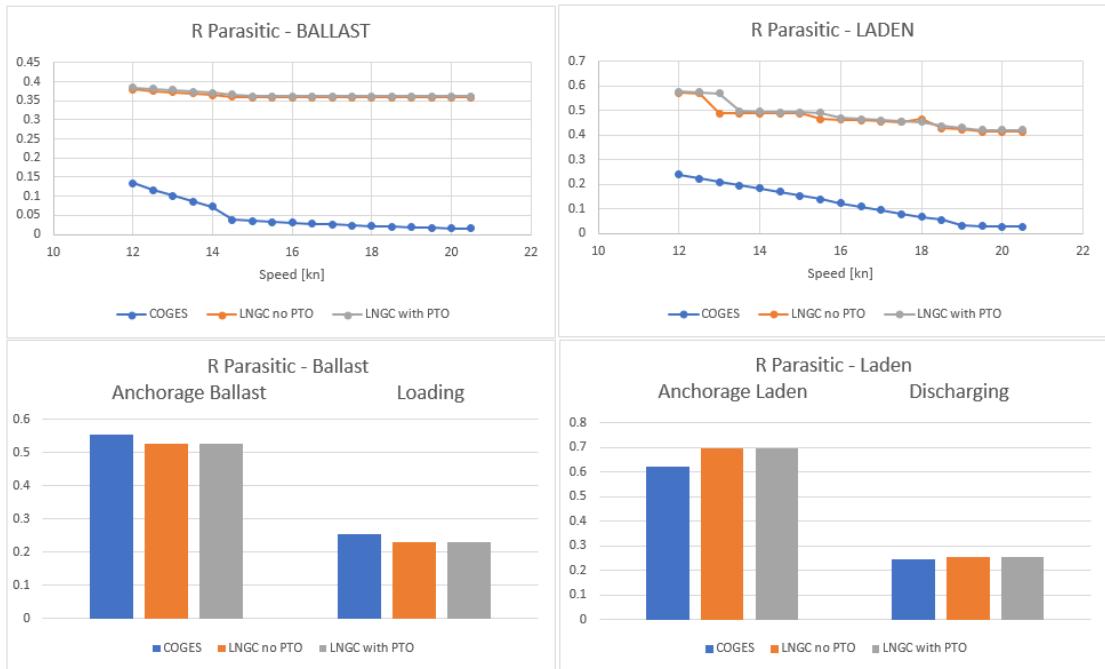


Figure 27: R Parasitic

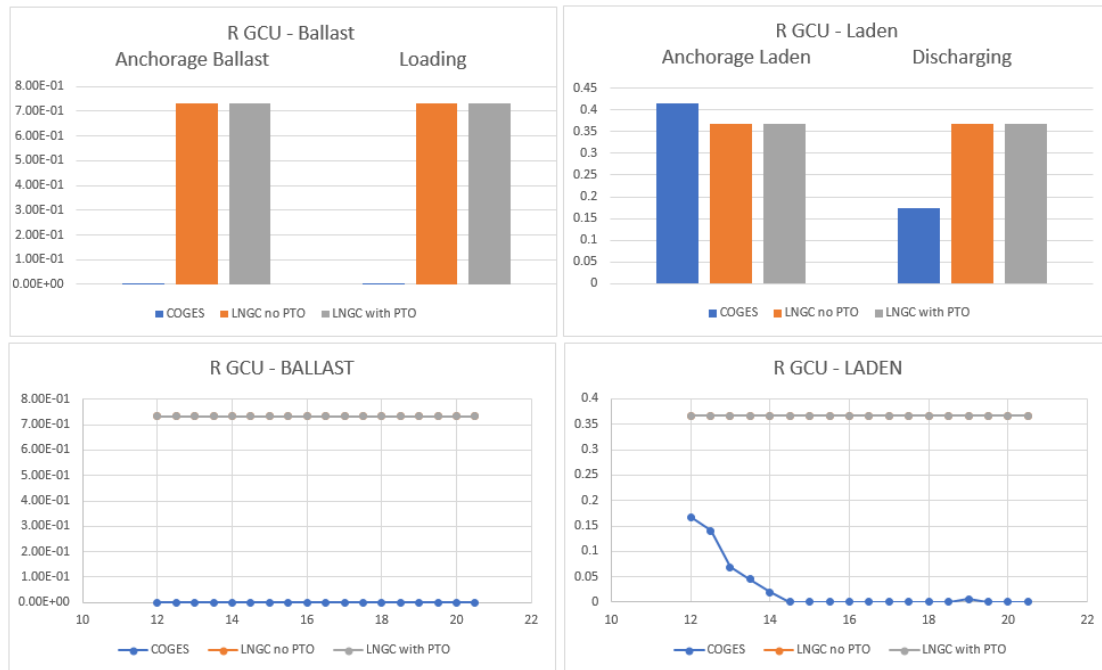


Figure 28: R GCU

These results illustrate the vessel's overall performance across the full range of operating speeds, as well as its non-sailing modes. The simulation results reveal several key differences between the COGES system and the two conventional LNG carrier configurations (with shaft generator and without). Firstly, the COGES-powered vessel exhibits higher cargo consumption per day. Despite this, the total energy consumption across the different ship types remains comparable; it is important to note that the COGES system operates without the use of pilot fuel, which contributes to this parity. Furthermore, while the COGES configuration demonstrates improved system efficiency at lower sailing speeds, largely due to its combined cycle operation, it exhibits lower overall ship efficiency when averaged across the full speed range. The COGES system model provides more optimal results compared to the two LNGC models only at  $r_{propulsion}$ ,  $r_{parasitic}$  and  $r_{GCU}$  coefficients. In the hope of an overall comparison of the three models, the performance results as a function of speed are adjusted to reflect two representative operational profiles.

# Initial Test Comparisons through the Roundtrips

## Analysis of the Roundtrips

The three simulations are being put to test in two different trips. For each trip there are accurate and realistic data regarding the time, the distance and the hours spent at each sailing speed ranging from 12 to 20 knots at ballast and laden condition. The time that the ship spends loading and unloading upon arrival and departure in the port is also taken into account in the calculations. The following figures are based on statistical data collected from actual voyages.

The first trip is between the USA and Europe as shown below. The total distance is 5,200 nm and the duration of the roundtrip is 736 hours.

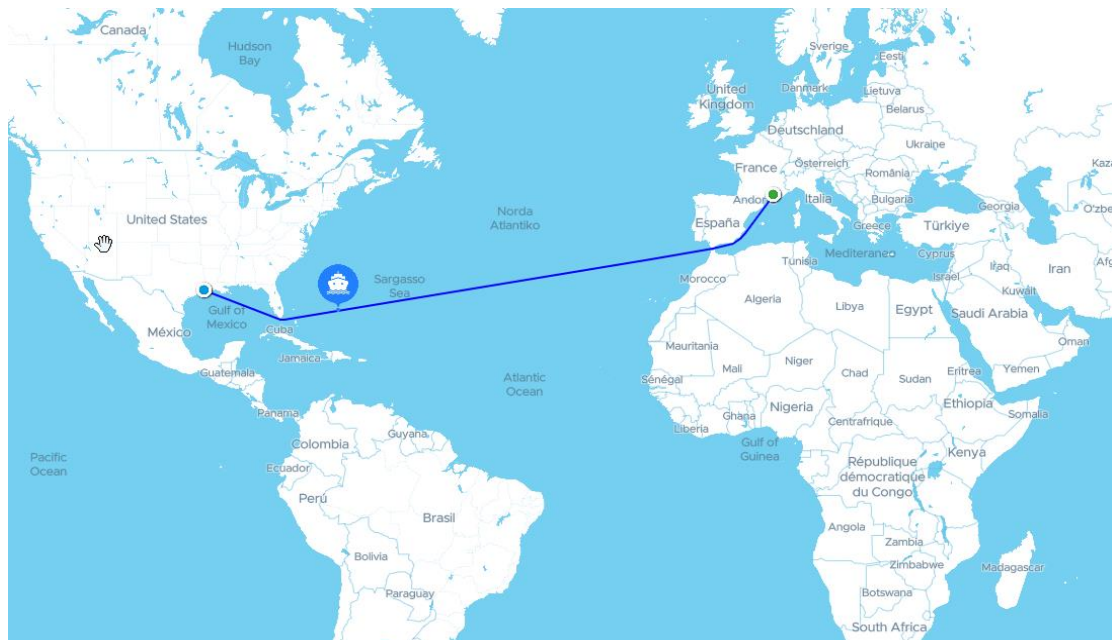


Figure 29: USA - Europe Trip

Table 20: Table of time spent on each velocity for the USA-EU Trip

<b>Mode</b>	<b>Index</b>	<b>Speed</b>	<b>hours</b>	<b>days</b>
Anch. Ballast	1	0	25.55	1.06
Loading	2	0	20.40	0.85
Laden	3	12	5.48	0.23
Laden	4	12.5	1.22	0.05
Laden	5	13	10.24	0.43
Laden	6	13.5	1.55	0.06
Laden	7	14	19.26	0.80
Laden	8	14.5	3.68	0.15
Laden	9	15	52.57	2.19
Laden	10	15.5	13.85	0.58
Laden	11	16	73.90	3.08
Laden	12	16.5	13.19	0.55
Laden	13	17	58.47	2.44
Laden	14	17.5	10.08	0.42
Laden	15	18	40.43	1.68
Laden	16	18.5	6.14	0.26
Laden	17	19	8.11	0.34
Laden	18	19.5	1.38	0.06
Laden	19	20	3.84	0.16
Anch. Loaded	20	0	25.14	1.05
Unloading	21	0	24.41	1.02
Ballast	22	12	6.89	0.29
Ballast	23	12.5	1.17	0.05
Ballast	24	13	13.94	0.58
Ballast	25	13.5	1.74	0.07
Ballast	26	14	18.13	0.76
Ballast	27	14.5	4.03	0.17
Ballast	28	15	47.08	1.96
Ballast	29	15.5	10.51	0.44
Ballast	30	16	50.13	2.09
Ballast	31	16.5	8.03	0.33
Ballast	32	17	51.09	2.13
Ballast	33	17.5	7.46	0.31
Ballast	34	18	30.70	1.28
Ballast	35	18.5	4.98	0.21
Ballast	36	19	43.27	1.80
Ballast	37	19.5	5.55	0.23
Ballast	38	20	12.03	0.50

In this operational profile, the vessel completes almost 12 roundtrips per year.

The second trip is between the USA and Asia. The total distance is 10,500 nm and the duration of the roundtrip is 1437 hours.

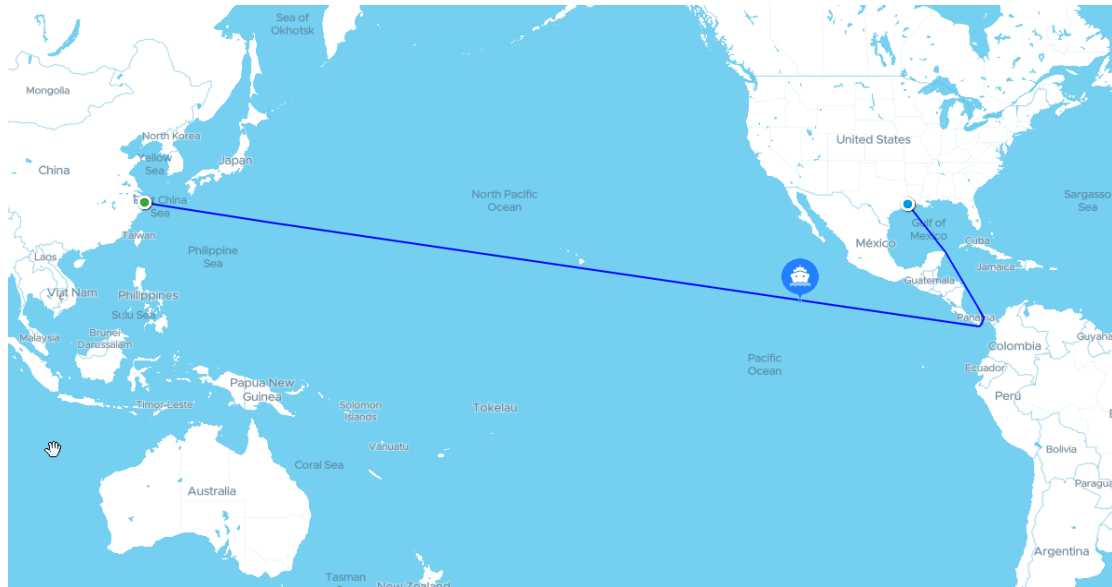


Figure 30: USA - Asia Trip

Table 21: Table of time spent on each velocity for the USA-Asia Trip

Mode	Index	Speed	hours	days
Anch. Ballast	1	0	40.46	1.69
Loading	2	0	21.39	0.89
Laden	3	12	18.92	0.79
Laden	4	12.5	3.53	0.15
Laden	5	13	36.45	1.52
Laden	6	13.5	5.24	0.22
Laden	7	14	66.37	2.77
Laden	8	14.5	4.81	0.20
Laden	9	15	100.99	4.21
Laden	10	15.5	19.78	0.82
Laden	11	16	180.49	7.52
Laden	12	16.5	62.09	2.59
Laden	13	17	111.68	4.65
Laden	14	17.5	19.35	0.81
Laden	15	18	33.03	1.38
Laden	16	18.5	1.82	0.08
Laden	17	19	6.95	0.29
Laden	18	19.5	1.39	0.06
Laden	19	20	1.39	0.06
Anch. Loaded	20	0	10.79	0.45
Unloading	21	0	27.16	1.13
Ballast	22	12	23.19	0.97
Ballast	23	12.5	6.76	0.28

Ballast	24	13	11.89	0.50
Ballast	25	13.5	3.68	0.15
Ballast	26	14	8.81	0.37
Ballast	27	14.5	11.89	0.50
Ballast	28	15	102.28	4.26
Ballast	29	15.5	108.96	4.54
Ballast	30	16	139.26	5.80
Ballast	31	16.5	21.14	0.88
Ballast	32	17	81.74	3.41
Ballast	33	17.5	13.95	0.58
Ballast	34	18	57.60	2.40
Ballast	35	18.5	8.81	0.37
Ballast	36	19	44.25	1.84
Ballast	37	19.5	5.73	0.24
Ballast	38	20	13.43	0.56

In this operational profile, the vessel completes a little further than 6 roundtrips per year.

### Initial Test Results

In order to understand better the results of the simulation in the two operational profiles explained above, there have been included three coefficients in the overall calculations.

- $\frac{\text{Energy consumed per Trip}}{\text{Cargo Volume transported} \times \text{Nautical Miles}}$
- $\frac{\text{Fuel Oil consumed per Trip}}{\text{Cargo Volume transported} \times \text{Nautical Miles}}$
- $\frac{\text{CO}_2 \text{ Emissions per Trip}}{\text{Cargo Volume transported} \times \text{Nautical Miles}}$

The results for the two roundtrips are shown in the following tables:

COGES	LNGC no PTO	LNGC with PTO
Cargo Delivered per year [tons]		
2050689	2051796	2052455
Energy per cbm transported x miles [MJ/m <sup>3</sup> nm]		
0.0010822	0.0010745	0.0010355
F. O. C. per cbm transported x miles [kg/m <sup>3</sup> nm]		
0.00193	0.00173	0.00167
CO2 per cbm transported x miles [kg/m <sup>3</sup> nm]		
0.0053	0.0048	0.0046

Table 22: Results for the USA - Europe Trip

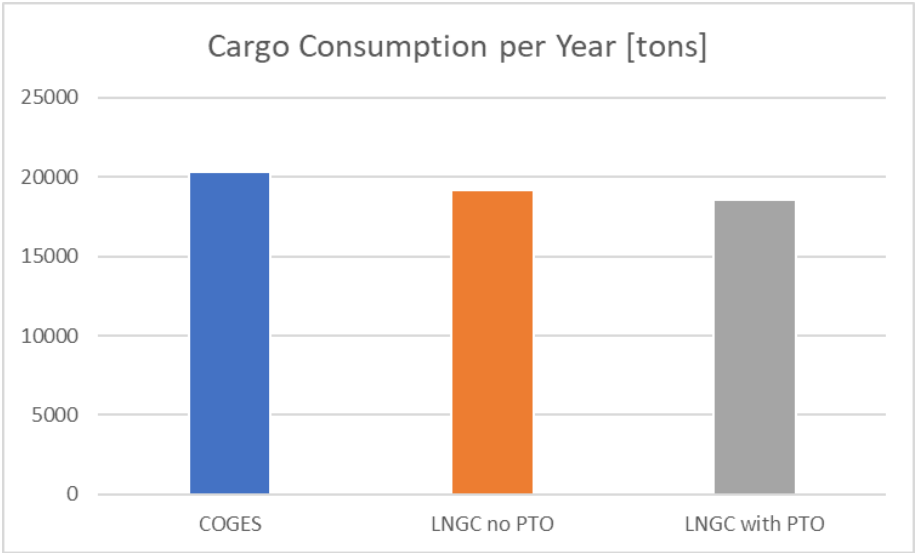


Figure 31: Cargo Consumption per Year (USA - EU Trip)

COGES	LNGC no PTO	LNGC with PTO
Cargo Delivered per year [tons]		
1040999	1041855	1042581
Energy per cbm transported x miles [MJ/m <sup>3</sup> nm]		
0.0868683	0.0859672	0.0824842
F. O. C. per cbm transported x miles [kg/m <sup>3</sup> nm]		
0.00181	0.00165	0.00158
CO2 per cbm transported x miles [kg/m <sup>3</sup> nm]		
0.0050	0.0045	0.0044

Table 23: Results for the USA - Asia Trip

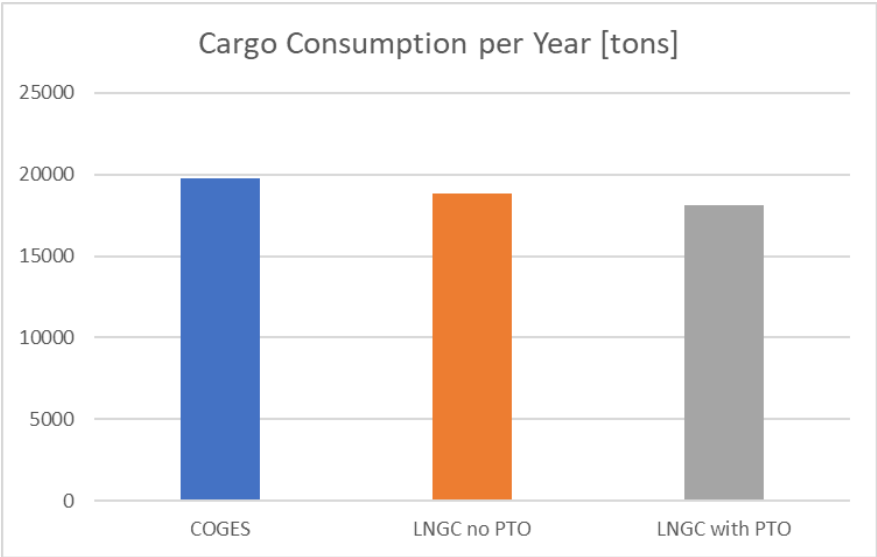


Figure 32: Cargo Consumption per Year (USA - ASIA Trip)

As the results indicate, the least efficient model in both operational profiles is the COGES powered vessel. More specifically, the ship with the COGES system delivers 0.09% and 0.15% less cargo than the conventional LNGC with shaft generator and consumes 4.51% and 5.32% more energy in the two trips respectively. As far as the CO<sub>2</sub> emissions are concerned, the COGES system emits 15.01% and 14.16% more CO<sub>2</sub>. Overall, the results show that this COGES configuration cannot replace the traditional two-stroke Dual Fuel engine.

## **Analysis of COGES System's Alterations**

Following the initial comparison between the COGES configuration and two conventional LNG carrier models, one with a shaft generator and one without, it was evident that while COGES presented some environmental advantages, the overall performance was in terms of efficiency and fuel consumption not yet optimal. To enhance the viability of the COGES system, several theoretical improvements were investigated based on its inherent characteristics.

Firstly, due to the more compact nature of the COGES arrangement compared to large two-stroke engines, the engine room occupies significantly less volume. This space-saving design presents the opportunity to increase the vessel's total cargo capacity without altering its external dimensions. In turn, this could improve the economic viability of the ship by enabling larger quantities of LNG to be transported per voyage. Secondly, the reduction of the machinery space allows for greater flexibility in hull design. With fewer constraints imposed by the propulsion layout, the ship's hull form can be optimized to reduce hydrodynamic resistance. This optimization translates to reduced propulsion power demand for the same operational speed, improving the overall energy efficiency of the vessel. Lastly, gas turbine performance plays a crucial role in the effectiveness of the COGES system. Advances in turbine technology have led to higher efficiencies, and exploring the impact of such improvements can provide insights into the long-term potential of the system. Therefore, various scenarios were developed to assess the effect of increasing gas turbine efficiency beyond the baseline value used in the first simulation.

To quantify the potential improvements discussed above, a set of parametric simulations were carried out. The first set of modifications concerns the ship's cargo capacity. Two cases were examined where the total cargo volume was increased by 5% and 10%, respectively. These values reflect the additional space made available by the reduced machinery footprint of the COGES system. The second set of simulations focused on hull form optimization. By assuming a more efficient hull design enabled by the compact configuration, reductions in total hull resistance were estimated at 2.5% and 5%. These reductions directly decrease the required propulsion power, thus lowering overall fuel consumption and improving energy efficiency. The third series of simulations addressed variations in gas turbine efficiency. Starting from a baseline efficiency of 0.3482, scenarios were run with improved values of 0.370, 0.375 and 0.395, representing incremental technological advancements or adoption of next-generation gas turbine units.

To capture the full benefit of the COGES system, a final set of simulations explored combinations of the above modifications. These combined cases aimed to assess the synergistic impact of increased cargo volume, reduced hull resistance, and improved gas turbine performance. The goal was to identify configurations where the cumulative advantages could yield a technoeconomically competitive alternative to conventional propulsion systems.

The analyses of these combined scenarios provide valuable insight into how design flexibility and technological advancements can make the COGES system not only environmentally favorable but also commercially viable. The increased cargo capacity, reduced propulsion energy requirements, and improved fuel efficiency make the COGES-equipped LNG carrier a strong contender for future fleet adoption, particularly in light of stricter emissions regulations and growing economic pressures.

## Presentation of Cases

### Cases Analysis

Among the various adaptations applied to the system and their respective combinations, a number of simulation cases were generated. In the following section, 12 of these cases are presented, as they yielded the most favorable results. The primary comparison between these cases is based on a set of key performance indicators, specifically:

- *Cargo Consumption per Year*
- *Total Energy Consumption per Year*
- *Cargo Delivered per Year*
- $\frac{\text{Energy Consumption per Year}}{\text{Cargo Volume transported} \times \text{Nautical Miles}}$  [Index A]
- $\frac{\text{Fuel Oil Consumption per Year}}{\text{Cargo Volume transported} \times \text{Nautical Miles}}$  [Index B]

In order to systematically present the modifications examined for the COGES configuration, three key parameters have been introduced, each corresponding to a specific design improvement. The increase in cargo volume is expressed as a percentage growth from the reference configuration, ranging from 0% to 10%, and is denoted as CVI (Cargo Volume Increase). The reduction of hydrodynamic resistance, which directly affects the required propulsion power, is represented as a percentage decrease in propulsion demand from 0% to 5%, and is symbolized as  $\alpha$ . Lastly, the performance of the gas turbine is described through its isentropic efficiency, starting from the base value of 0.348 and increasing to a maximum realistic value of 0.395. this parameter is referred to as  $n_{GT}$ . These symbols will be consistently used in the following sections to describe individual and combined simulation scenarios. It is important to highlight that the following cases are evaluated in relation to the initial test results and every percentage difference refers to the comparison between COGES and LNGC with PTO.

## Case 1

- $a=0\%$
- $CVI=0\%$
- $n_{GT} = 0.375$

In the first case, there is an energy equivalent of Total Energy Consumption per Year with 1.39% and 1.09% improvement at the two roundtrips although the Cargo Consumption per Year shows 3.96% and 3% worse values in the comparison between COGES and LNGC with PTO.

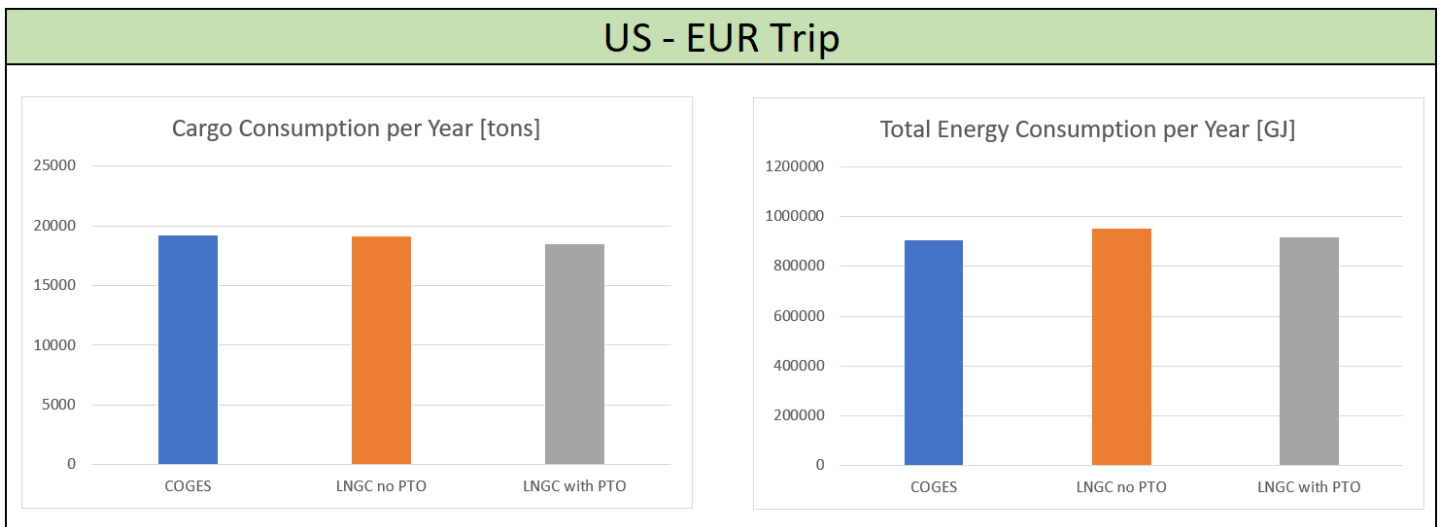


Figure 33: Case 1 Results for US-EUR Trip

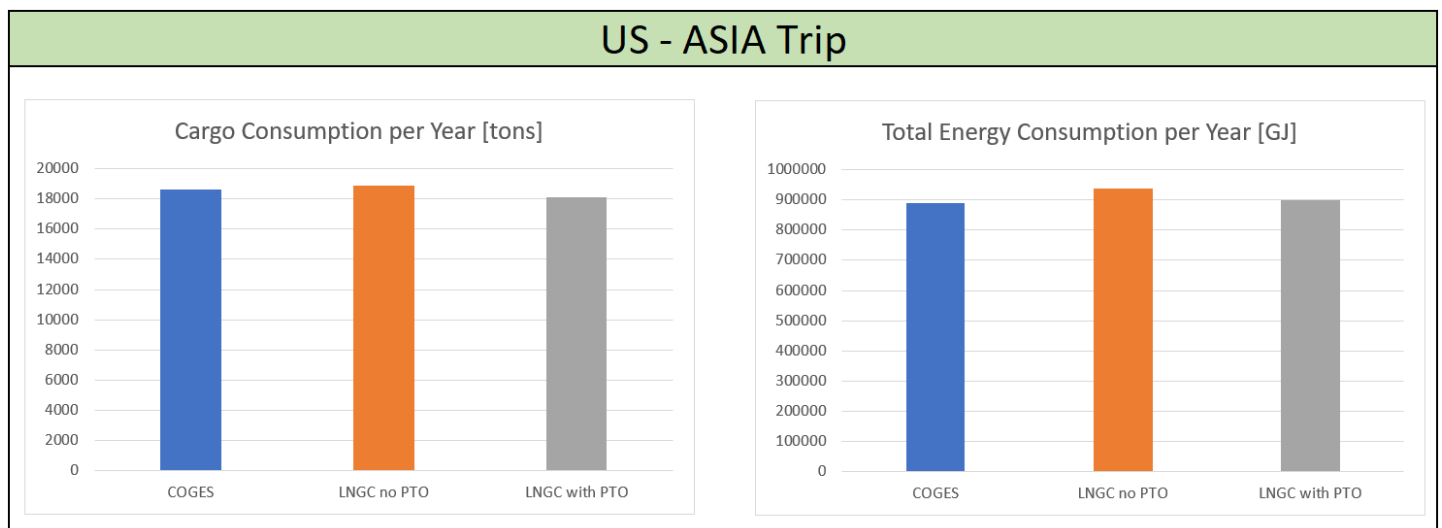


Figure 34: Case 1 Results for US - ASIA Trip

## Case 2

- $a=0\%$
- $CVI=0\%$
- $n_{GT} = 0.395$

The second case, which includes the highest realistic value of the gas turbine's performance (39.5%), shows a 5.3% reduction of Total Energy Consumption per Year while keeping almost the same Cargo Consumption per Year (-0.74% and 1% difference for the two operational profiles).

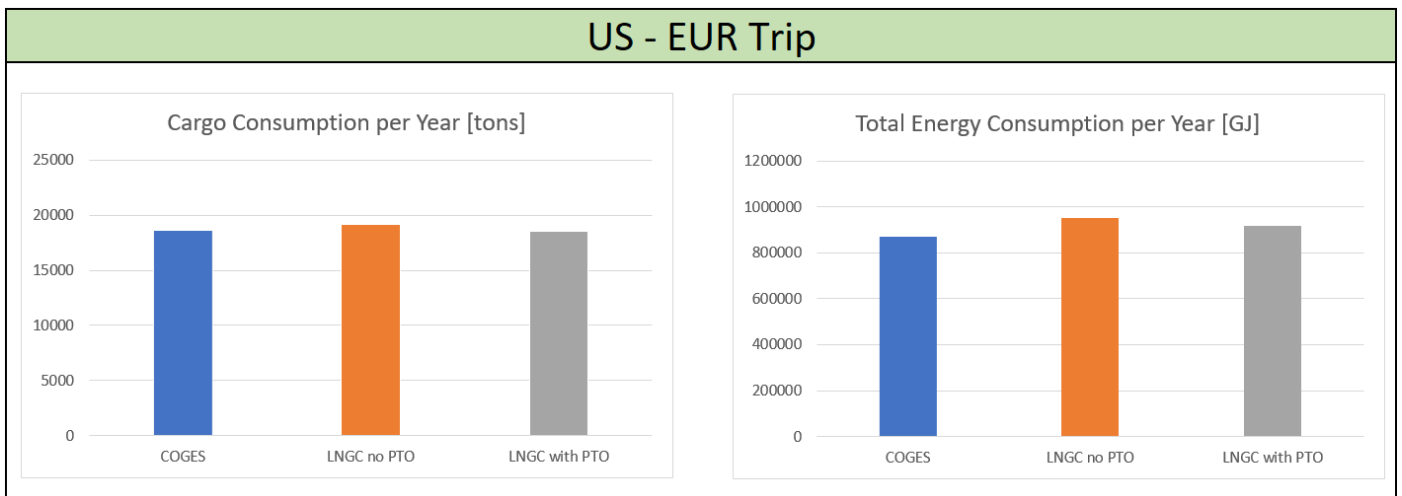


Figure 35: Case 2 Results for US-EUR Trip

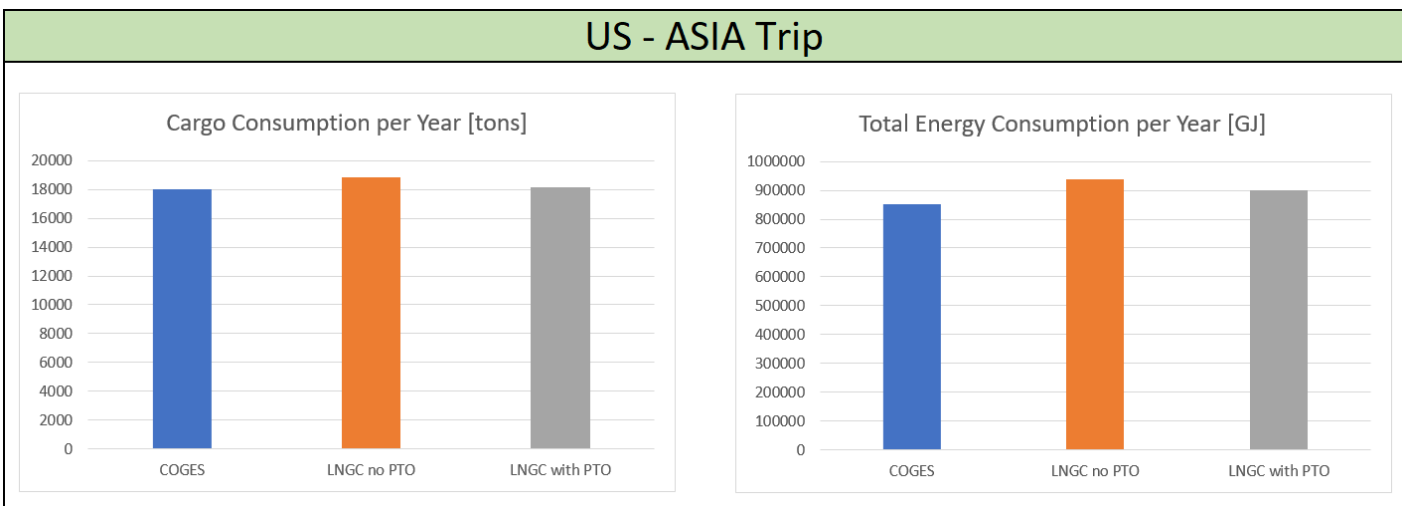


Figure 36: Case 2 Results for US - ASIA Trip

### Case 3

- a=0%
- CVI=5%
- $n_{GT} = 0.348$

This case presents the model only with the modification of the total cargo volume increase of 5%. The simulation indicates a 4.9% increase of the total cargo delivered per year, 11% and 10% more cargo consumption per year and 0.06% and 0.8% worse values for index A in the two trips.

US - EUR Trip			US - ASIA Trip		
COGES	LNGC no PTO	LNGC with PTO	COGES	LNGC no PTO	LNGC with PTO
Cargo Delivered per year [tons]					
2153921	2051796	2052455	1093726	1041855	1042581
4.9%			4.9%		
Energy per cbm transported x miles [MJ/m <sup>3</sup> nm]					
0.0871	0.0903	0.0870	0.0831	0.0860	0.0825
0.06%			0.80%		

Table 24: Case 3 Results

### Case 4

- a=0%
- CVI=10%
- $n_{GT} = 0.348$

In the fourth case, which considers a 10% increase in total cargo capacity, the results show a 10% rise in annual cargo delivered, an improvement of 13.09% in index A, and an average enhancement of 3.5% in index B.

US - EUR Trip			US - ASIA Trip		
COGES	LNGC no PTO	LNGC with PTO	COGES	LNGC no PTO	LNGC with PTO
Cargo Delivered per year [tons]					
2258364	2051796	2052455	1147634	1041855	1042581
10.03%			10.08%		
Energy per cbm transported x miles [MJ/m <sup>3</sup> nm]					
0.0756	0.0903	0.0870	0.0717	0.0860	0.0825
13.09%			13.09%		
F. O. C. per cbm transported x miles [kg/m <sup>3</sup> nm]					
0.0017	0.0018	0.0018	0.0016	0.0017	0.0017
3.25%			3.99%		

Table 25: Case 4 Results

## Case 5

- $a=2.5\%$
- $CVI=0\%$
- $n_{GT} = 0.348$

Case 5 and 6 present two models with improved hull form and reduced resistance. Case 5, which considers a 2.5% reduction on the ship's resistance, shows an average of 7% more cargo consumption and 3% more total energy consumption per year on the two trips.

US - EUR Trip			US - ASIA Trip		
COGES	LNGC no PTO	LNGC with PTO	COGES	LNGC no PTO	LNGC with PTO
Cargo Delivered per year [tons]					
19974	19182	18523	19407	18855	18129
-7.83%			-7.05%		
Total Energy Consumption per year [GJ]					
942294.7	952791.1	918191.5	930507.7	938307.0	900290.4
-2.63%			-3.36%		

Table 26: Case 5 Results

## Case 6

- $a=5\%$
- $CVI=0\%$
- $n_{GT} = 0.348$

In the sixth case, where a 5% reduction on the total resistance is displayed, the results show an average of 6% more cargo consumption and 1% more total energy consumption per year on each trip.

US - EUR Trip			US - ASIA Trip		
COGES	LNGC no PTO	LNGC with PTO	COGES	LNGC no PTO	LNGC with PTO
Cargo Delivered per year [tons]					
19664	19182	18523	19120	18855	18129
-6.16%			-5.47%		
Total Energy Consumption per year [GJ]					
926951.4	952791.1	918191.5	915635.3	938307.0	900290.4
-0.95%			-1.70%		

Table 27: Case 6 Results

## Case 7

- $a=0\%$
- $CVI=5\%$
- $n_{GT} = 0.395$

The set of the two following cases presents two models with a combination of cargo volume increase and improved values for the gas turbine efficiency. The features of case seven are the following: 5% cargo volume increase and the highest realistic value of the gas turbine's performance (39.5%). The results show 4.8% less energy consumption per year, although the model consumes 2.5% more cargo per year, an average of 9.3% improvement on index A and 1.7% and 2.7% improvement on index for each operational profile.

US - EUR Trip			US - ASIA Trip		
COGES	LNGC no PTO	LNGC with PTO	COGES	LNGC no PTO	LNGC with PTO
Total Energy Consumption per Year [GJ]					
873963	952791	918192	856593	938307	900290
4.82%			4.85%		
Energy per cbm transported x miles [MJ/m <sup>3</sup> nm]					
0.0789	0.0903	0.0870	0.0747	0.0860	0.0825
9.35%			9.38%		
F. O. C. per cbm transported x miles [kg/m <sup>3</sup> nm]					
0.0017	0.0018	0.0018	0.0016	0.0017	0.0017
1.71%			2.70%		

*Table 28: Case 7 Results*

## Case 8

- $a=0\%$
- $CVI=10\%$
- $n_{GT} = 0.37$

Case 8 presents a model equipped with a gas turbine with an efficiency equal to 0.37 and a cargo volume 10% more than the original model. The results of case 8 indicate 10% more cargo delivered per year, an average of 8.3% improvement on index A and 0.27-1.06% improvement on index B.

US - EUR Trip			US - ASIA Trip		
COGES	LNGC no PTO	LNGC with PTO	COGES	LNGC no PTO	LNGC with PTO
Cargo Delivered per year [tons]					
2257756	2051796	2052455	1147051	1041855	1042581
10.00%			10.02%		
Energy per cbm transported x miles [MJ/m <sup>3</sup> nm]					
0.0795	0.0903	0.0870	0.0757	0.0860	0.0825
8.58%			8.26%		
F. O. C. per cbm transported x miles [kg/m <sup>3</sup> nm]					
0.0018	0.0018	0.0018	0.0016	0.0017	0.0017
0.27%			1.06%		

Table 29: Case 8 Results

## Cases 9-12

The last four cases are being presented together, because they contain the four possible combinations of cargo volume increase and reduction of the hull's resistance.

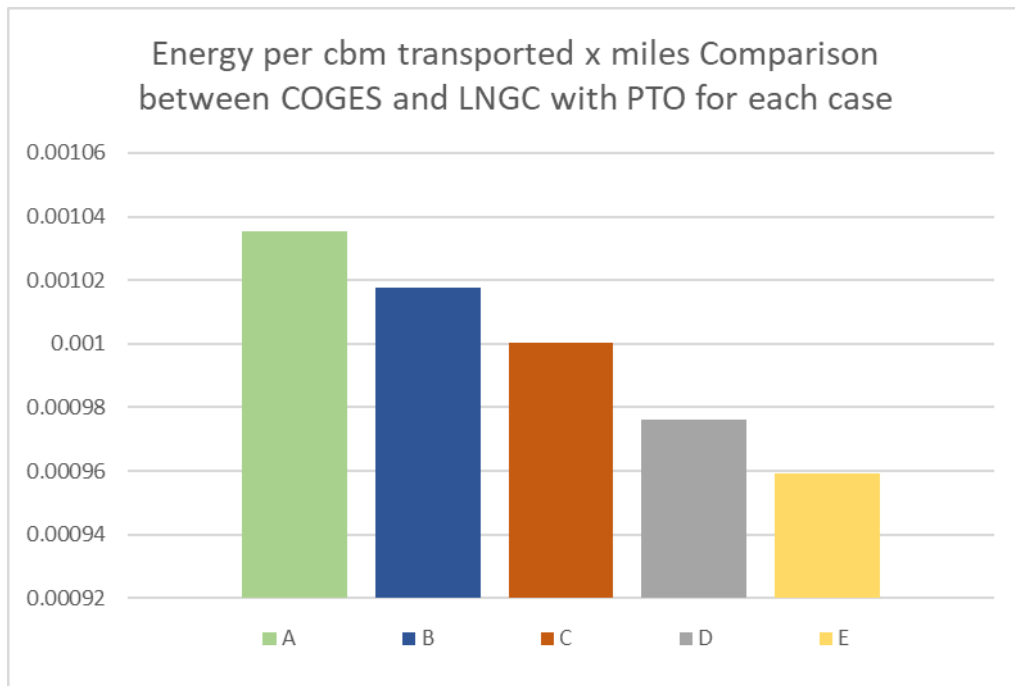
Case 9	Case 10	Case 11	Case 12
a=2.5%	a=5%	a=2.5%	a=5%
CVI=5%	CVI=5%	CVI=10%	CVI=10%

Figure 37: Features of Cases 9-12

The last four scenarios are grouped according to each specific voyage, with the resulting data summarized in the subsequent tables.

**US - EUR Trip**

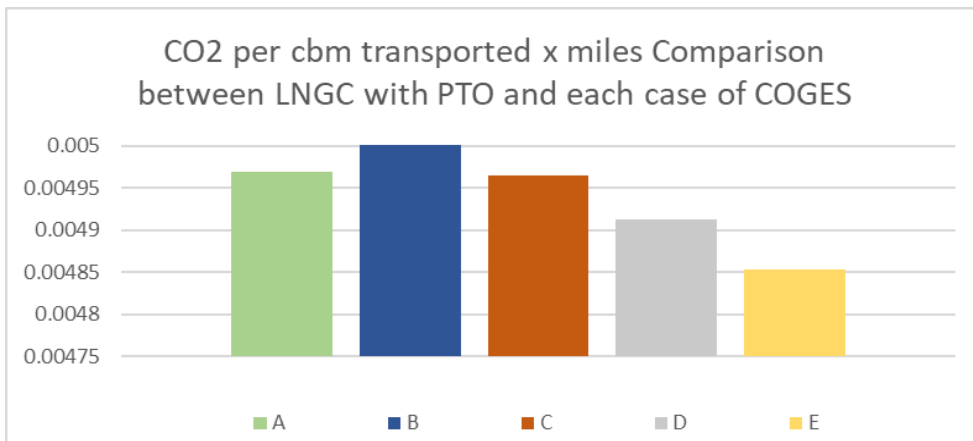
		5%			10%		
a	2.50%	Energy per cbm transported x miles [MJ/m <sup>3</sup> nm]			Energy per cbm transported x miles [MJ/m <sup>3</sup> nm]		
		COGES	LNGC no PTO	LNGC with PTO	COGES	LNGC no PTO	LNGC with PTO
	0.00101764	0.001074531	0.001035511	0.000976081	0.001074531	0.001035511	
	Difference between COGES and LNGC			1.76%	Difference between COGES and LNGC		
5%	5%	Energy per cbm transported x miles [MJ/m <sup>3</sup> nm]			Energy per cbm transported x miles [MJ/m <sup>3</sup> nm]		
		COGES	LNGC no PTO	LNGC with PTO	COGES	LNGC no PTO	LNGC with PTO
	0.00100047	0.001074531	0.001035511	0.000959267	0.001074531	0.001035511	
	Difference between COGES and LNGC			3.50%	Difference between COGES and LNGC		



A	LNG with PTO
B	a=2.5% C_V_I=5%
C	a=5% C_V_I=5%
D	a=2.5% C_V_I=10%
E	a=5% C_V_I=10%

Table 30: Case 9-12 Results for US - EUR Trip (1)

C_V_I		5%			10%		
a	2.50%	CO2 per cbm transported x miles [kg/m <sup>3</sup> nm]			CO2 per cbm transported x miles [kg/m <sup>3</sup> nm]		
		COGES	LNGC no PTO	LNGC with PTO	COGES	LNGC no PTO	LNGC with PTO
		0.00503816	0.005151845	0.004969639	0.004912498	0.005151845	0.004969639
		Difference between COGES and LNGC		-1.36%	Difference between COGES and LNGC		1.16%
5%	5%	CO2 per cbm transported x miles [kg/m <sup>3</sup> nm]			CO2 per cbm transported x miles [kg/m <sup>3</sup> nm]		
		COGES	LNGC no PTO	LNGC with PTO	COGES	LNGC no PTO	LNGC with PTO
		0.00496521	0.005151845	0.004969639	0.004853109	0.005151845	0.004969639
		Difference between COGES and LNGC		0.09%	Difference between COGES and LNGC		2.40%



A	LNG with PTO
B	a=2.5% C_V_I=5%
C	a=5% C_V_I=5%
D	a=2.5% C_V_I=10%
E	a=5% C_V_I=10%

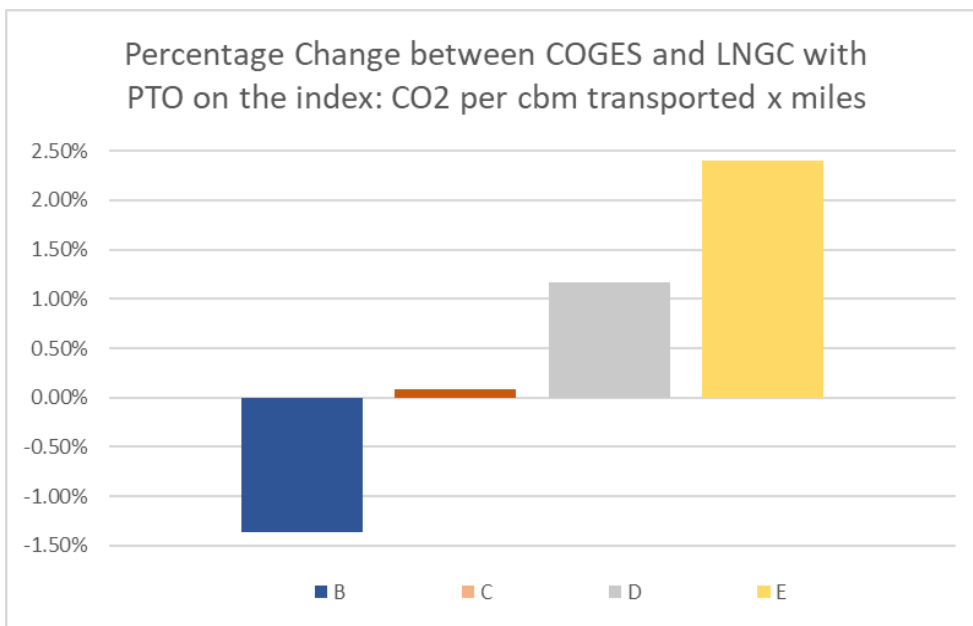


Table 31: Case 9-12 Results for US - EUR Trip (2)

**US - Asia Trip**

C_V_I		5%			10%		
a	2.50%	Energy per cbm transported x miles [MJ/m <sup>3</sup> nm]			Energy per cbm transported x miles [MJ/m <sup>3</sup> nm]		
		COGES	LNGC no PTO	LNGC with PTO	COGES	LNGC no PTO	LNGC with PTO
		0.081615824	0.085967245	0.082484176	0.07826992	0.085967245	0.082484176
		Difference between COGES and LNGC		1.06%	Difference between COGES and LNGC		5.38%
5%	5%	Energy per cbm transported x miles [MJ/m <sup>3</sup> nm]			Energy per cbm transported x miles [MJ/m <sup>3</sup> nm]		
		COGES	LNGC no PTO	LNGC with PTO	COGES	LNGC no PTO	LNGC with PTO
		0.080268951	0.085967245	0.082484176	0.07694702	0.085967245	0.082484176
		Difference between COGES and LNGC		2.76%	Difference between COGES and LNGC		7.20%

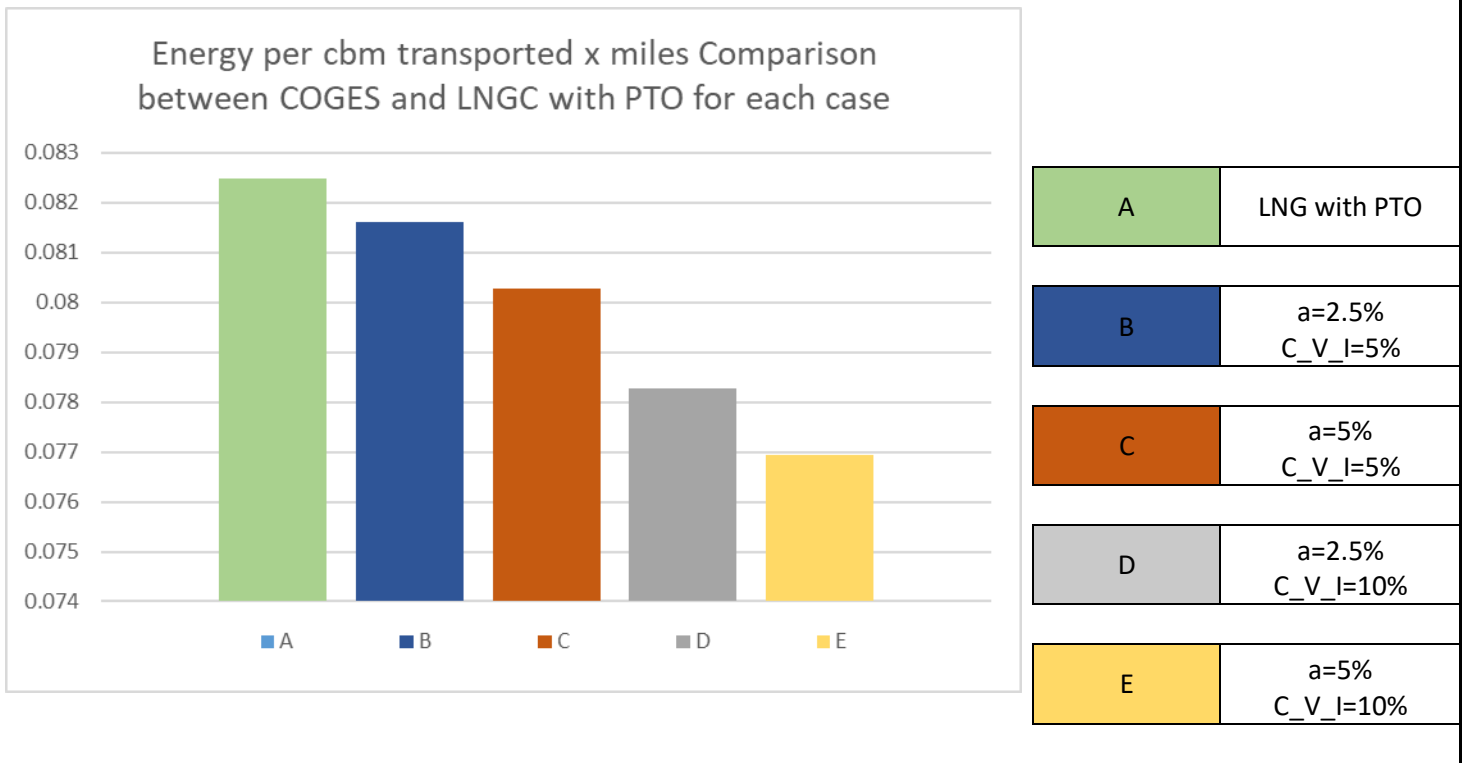
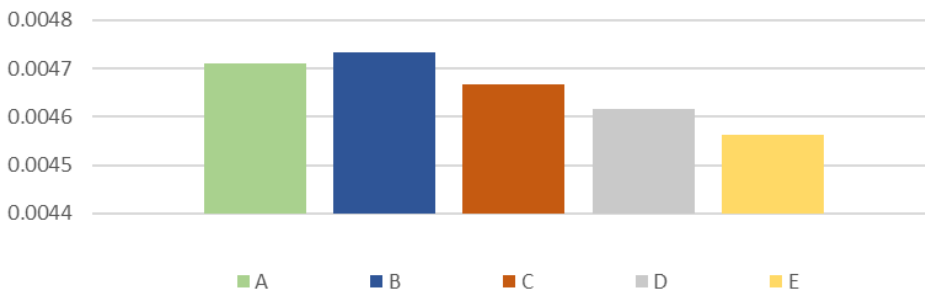


Table 32: Case 9-12 Results for US - ASIA Trip (1)

C_V_I		5%			10%		
a	2.50%	CO2 per cbm transported x miles [kg/m <sup>3</sup> nm]			CO2 per cbm transported x miles [kg/m <sup>3</sup> nm]		
		COGES	LNGC no PTO	LNGC with PTO	COGES	LNGC no PTO	LNGC with PTO
		0.004734049	0.004904127	0.004710776	0.00461591	0.004904127	0.004710776
	Difference between COGES and LNGC			-0.49%	Difference between COGES and LNGC		2.06%
5%	CO2 per cbm transported x miles [kg/m <sup>3</sup> nm]			CO2 per cbm transported x miles [kg/m <sup>3</sup> nm]			
	COGES	LNGC no PTO	LNGC with PTO	COGES	LNGC no PTO	LNGC with PTO	
	0.004667765	0.004904127	0.004710776	0.00456387	0.004904127	0.004710776	
Difference between COGES and LNGC			0.92%	Difference between COGES and LNGC		3.22%	

CO2 per cbm transported x miles Comparison between LNGC with PTO and each case of COGES



A	LNGC with PTO
B	a=2.5% C_V_I=5%
C	a=5% C_V_I=5%
D	a=2.5% C_V_I=10%
E	a=5% C_V_I=10%

Percentage Change between COGES and LNGC with PTO on the index: CO2 per cbm transported x miles

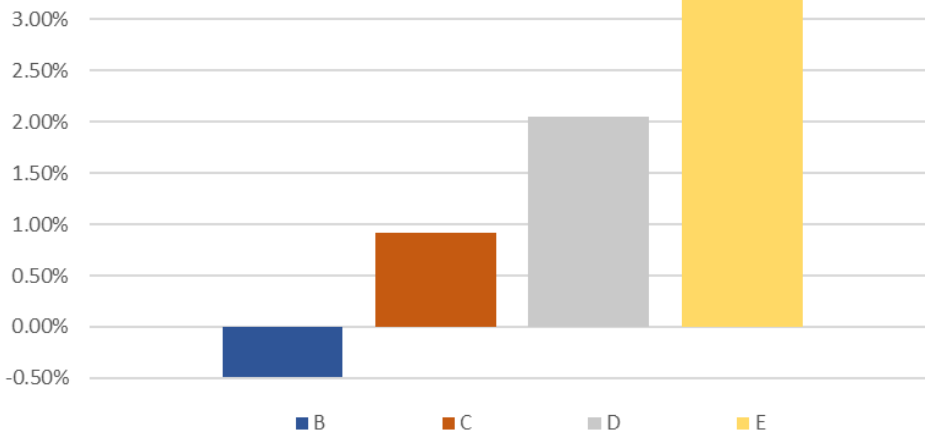


Table 33: Case 9-12 Results for US - ASIA Trip (2)

In Case 9, the introduction of a moderate hull resistance reduction (2.5%) and a 5% increase in cargo capacity leads to a 9.5% rise in annual cargo consumption and a 4.9% increase in cargo delivered compared to the conventional reference vessel. However, this comes at the cost of a 3.5% increase in total yearly energy consumption, resulting in a deterioration of index B. This suggests that the limited hydrodynamic improvement is not sufficient to offset the relatively high cargo fuel consumption, leading to poorer energy efficiency per transported unit.

With a more pronounced hull resistance reduction (5%) and the same 5% cargo volume increase as Case 9, Case 10 achieves a more favorable energy balance. The annual energy consumption rises only by 1.8%, while cargo delivered still improves by 4.9%. Despite a lower cargo consumption increase (7.5%), this case demonstrates a better trade-off between performance and fuel use, highlighting the significance of hydrodynamic optimization in COGES-based configurations.

Case 11 focuses on cargo volume expansion (10%) while retaining the moderate 2.5% hull resistance reduction. As expected, annual cargo consumption increases significantly (11%), and the amount of cargo delivered rises by 9.8%. However, the energy consumption increase (3.9%) remains relatively high, indicating that a larger cargo load alone, without sufficient efficiency gains, can increase operational energy requirements. Still, index A improves, owing to the substantially higher delivery volume.

Case 12 combines the highest hull resistance reduction (5%) with the largest cargo volume increase (10%), resulting in a 10% increase in delivered cargo and only a 2.3% rise in annual energy consumption. Consequently, it achieves the best performance in both index A and index B, confirming the strong synergistic effect of compact machinery layout and hydrodynamic improvements on operational efficiency.

When examining the four modified COGES configurations, it becomes evident that Case 12 consistently outperforms the others in terms of energy and fuel efficiency per unit of transported cargo. It effectively leverages both hydrodynamic advantages and spatial benefits offered by the compact system design. In contrast, Case 9, with only moderate hull resistance gains and limited cargo capacity expansion, exhibits the least favorable performance, even underperforming the conventional shaft-generator-based LNG carrier in terms of fuel consumption per cbm·nm. This highlights the risk of suboptimal integration of compact systems without corresponding improvements in hull form. Cases 10 and 11 represent intermediate scenarios. Case 10 demonstrates that improving hull resistance alone can lead to better overall efficiency, while Case 11 shows that cargo capacity expansion, even without aggressive resistance reduction, still contributes significantly to transport productivity but at a higher energy cost. Overall, the results underline that the combined application of hydrodynamic refinement and machinery compactness is essential to unlock the full potential of the COGES concept in LNG carriers.

## Conclusions

The steadily growing global demand for LNG is driving advancements in LNG carrier designs and their propulsion systems. Given the widespread applications of natural gas in everyday life and the current geopolitical landscape, LNG has become a highly valuable commodity, making its transportation methods a critical focus. The newly developed COGES system shows great potential in improving fuel efficiency and reducing carbon emissions. While it has not yet matched the performance of the widely used two-stroke dual-fuel engines, it offers shipowners the advantage of transporting significantly larger cargo volumes.

Out of the twelve evaluated cases, configurations incorporating a Cargo Volume Increase (CVI) consistently demonstrate superior operational performance by enabling greater transported cargo capacity relative to the conventional LNG carrier baseline. From a purely energetic standpoint, Cases 1 and 2 achieve the lowest absolute energy consumption figures, highlighting the critical importance of gas turbine efficiency. These results emphasize the industrial necessity to focus efforts on improving gas turbine performance to achieve meaningful energy savings. Furthermore, Cases 7 through 12 exhibit the most favorable energy efficiency metrics when normalized per unit of transported cargo, indicating a reduced energy footprint. These findings are critical in the context of the IMO's decarbonization regulations and the global Net-Zero emissions targets, which drive the maritime industry toward minimizing greenhouse gas (GHG) emissions. It is important to note that the trends observed for energy consumption directly translate to GHG emissions, with cases exhibiting lower energy footprints also achieving reduced CO<sub>2</sub> emissions per transported volume and distance. Thus, optimizing hull hydrodynamics and machinery compactness to increase cargo capacity plays a pivotal role in meeting stringent environmental standards and advancing sustainable LNG carrier operations.

New LNG carriers are being constructed daily, with COGES propulsion systems ready for integration into these vessels. According to BRS, more than 240 new LNG carriers will need to be built by 2034 to meet the global demand for natural gas (*Hlne*, 2025). A comprehensive technoeconomic assessment can clearly highlight the differences in total annual profitability between COGES-powered ships and conventional LNG carriers. Such an evaluation is likely to motivate shipowners to invest in the COGES technology, demonstrating that this approach is among the most effective solutions moving forward. As the industry transitions toward the NET ZERO era, COGES systems stand out as some of the most promising technologies to bridge the gap in the rapidly evolving LNG transportation sector.

## References

- Dimopoulos, G., Georgopoulou, C., Stefanatos, J. (2019). *Advanced Ship Machinery Modeling and Simulation*. [https://doi.org/10.1007/978-3-030-02810-7\\_14](https://doi.org/10.1007/978-3-030-02810-7_14)
- G70ME-C10\_5-GI*.(2025). [https://man-es.com/applications/projectguides/2stroke/content/printed/G70ME-C10\\_5-GI.pdf](https://man-es.com/applications/projectguides/2stroke/content/printed/G70ME-C10_5-GI.pdf)
- Global Maritime Forum*. (2023). <https://globalmaritimeforum.org/insight/the-implications-of-the-imo-revised-ghg-strategy-for-shipping/>
- gPROMS Digital Process Design and Operation*. (2025). <https://www.siemens.com/global/en/products/automation/industry-software/gproms-digital-process-design-and-operations.html>
- Hlne*. (n.d.). <https://www.tradewindsnews.com/gas/over-240-lng-newbuildings-needed-by-2034-to-meet-global-demand-says-brs/2-1-1797550>
- IMO*. (2024). <https://www.imo.org/en/MediaCentre/PressBriefings/pages/MEPC-82-makes-progress-IMO-netzero-framework.aspx>
- LNG Composition*. (2024). <https://www.nationalgrid.com/stories/energy-explained/what-is-liquefied-natural-gas-lng#:~:text=Clear%2C%20odourless%20and%20colourless%2C%20LNG,on%20its%20sou>
- MEGI Two Stroke Engines*. (2025). <https://www.man-es.com/marine/products/two-stroke-engines/me-gi>
- Methane Pioneer: The First LNG Ship in the World*. (2012). <https://www.marineinsight.com/types-of-ships/methane-pioneer-the-first-lng-ship-in-the-world/>
- Methane Slip*. (n.d.). <https://www.wartsila.com/marine/services/lifecycle-upgrades/methane-slip-reduction-solutions>

*SGT-400 gas turbine.* (2025). <https://www.siemens-energy.com/global/en/home/products-services/product/sgt-400.html#/>

*Wärtsilä 31SG.* (2025). <https://www.wartsila.com/marine/products/engines-and-generating-sets/pure-gas-engines/wartsila-31sg>

*Wärtsilä 34DF Product guide.* (2017).

*Wärtsilä Shaft Generators.* (n.d.). [https://www.wartsila.com/marine/products/ship-electrification-solutions/shaft-generator?utm\\_source=organic&utm\\_medium=MP-press-release&utm\\_term=marine-power&utm\\_content=shaft-generator&utm\\_campaign=Wartsila-shaft-generator-systems-will-deliver-fuel-saving](https://www.wartsila.com/marine/products/ship-electrification-solutions/shaft-generator?utm_source=organic&utm_medium=MP-press-release&utm_term=marine-power&utm_content=shaft-generator&utm_campaign=Wartsila-shaft-generator-systems-will-deliver-fuel-saving)

*X-DF Dual-Fuel Design.* (2025). <https://wingd.com/design-development/engine-technologies/x-df-dual-fuel-design>









